Appl. Math. J. Chinese Univ.
2026, 41(1): 225-254

Fractional calculus approach to RT-IN enzymatic competition in modulating HIV replication dynamics

Tushar Ghosh[1] Oluwole Daniel Makinde[2]
WANG Shu[3] Priti Kumar Roy[1,*]

Abstract. HIV infection continues to pose a significant global health challenge, with sub-Saharan Africa bearing a disproportionate burden. The replication cycle of HIV is fundamentally driven by intricate molecular interactions. This study investigates the competitive biochemical interplay between reverse transcriptase (RT) and integrase (IN) enzymes, employing a fractional calculus framework to model their mutual inhibitory effects. Through the application of fixed-point theory and Picard stability analysis, the existence, uniqueness, and stability of the fractional-order system are rigorously established. The role of RT-IN enzymatic competition in influencing HIV replication dynamics is elucidated through global sensitivity analysis using Latin Hypercube Sampling. Furthermore, the model incorporates memory-dependent characteristics by examining three distinct fractional operators, namely, the Caputo, Caputo-Fabrizio, and Atangana-Baleanu operators in the Caputo sense, thereby elucidating their respective influences on system behavior. The Atangana-Baleanu operator, in particular, demonstrates an enhanced capacity to capture the complex, synergistic processes underpinning HIV progression. This research provides a critical nexus between molecular virology and applied mathematics, offering foundational insights for the advancement of more precise and targeted therapeutic strategies against HIV.

§1 Introduction

HIV remains a serious and widespread concern in global public health. According to WHO statistical data, at the end of 2023, 39.9 million [36.1-44.6 million] people were living with HIV [1]. The African region is the most affected, with one in every 30 adults living with HIV [1]. In

Received: 2025-03-28. Revised: 2025-06-30.
MR Subject Classification: 92-XX, 44-XX, 37-XX, 34A08.
Keywords: HIV, biochemical interaction, physical interaction, fractional calculus, Sumudu transformation, LHS, PRCC.
Digital Object Identifier(DOI): https://doi.org/10.1007/s11766-026-5417-8.
Supported by the DST FIST Programme (SR/FST/MS-II/2021/101(C)) and UGC-JRF (21161010788). WANG Shu is supported by NSFC (11831003, 12171111) and SFC (KZ202110005011).
*Corresponding author.

East and Southern Africa, the burden of HIV is particularly severe, with approximately 20.8 million people affected [2]. South Africa alone accounts for a significant proportion, with 7.5 million people living with HIV [2]. In the HIV replication process, molecular interactions play a crucial role. These interactions are not only essential for viral replication but also serve as key targets in the development of effective antiretroviral therapies. This study focuses on two critical molecular interactions: the physical and biochemical interactions between the reverse transcriptase (RT) and integrase (IN) enzymes.

In the HIV replication process, the RT converts single-stranded RNA (ssRNA) to double-stranded DNA (dsDNA), also known as viral DNA, with the assistance of its two subunits (p66 and p51 [3]). Subsequently, the IN enzyme binds to the RT-synthesized viral DNA, forming a complex known as the pre-integration complex (PIC). The formation and stabilization of the PIC are essential for integrating viral DNA into the host genome during HIV replication. Within the PIC, viral DNA acts as the donor for integration into the host genome, a process catalyzed by the IN enzyme and referred to as auto-integration [4]. Concurrently, the physical interaction occurs when the RT enzyme binds to the C-terminal domain of the IN enzyme, thereby inhibiting the auto-integration process and ensuring effective viral integration [5, 6]. These molecular interactions are described in detail in the schematic diagram Fig. 1.

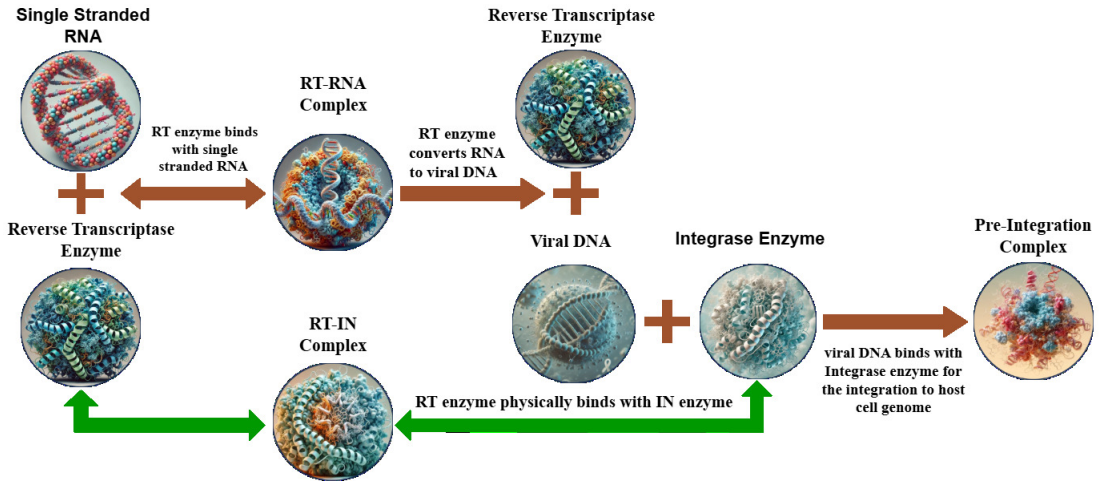

Figure 1. This schematic diagram illustrates competitive relation of the biochemical and physical interactions between RT and IN enzymes during HIV replication. It highlights the molecular dynamics and enzymatic complexes formed during the viral life cycle, providing insights into their roles in replication and integration processes. Brown arrows are denotes the biochemical interactions while the green arrow are symbolized for physical interaction.

Molecular studies have shown promising results in the development of hybrid molecules that inhibit multiple targets including RT and IN enzymes. Researchers are increasingly focusing on molecular interactions to design more effective therapeutic regimens for HIV treatment. Recently, Liman et al. [7] investigated hybrid molecules as potential drugs for combating HIV infection, while Marra et al. [8] explored the role of macrophages and viral reservoirs in

developing novel treatment strategies. Chakraborty et al. [9] analyzed viral DNA expression within the PIC, considering both biochemical and physical interactions. Ghosh et al. [10] demonstrated the relative effect of the biochemical and physical interaction between RT and IN enzymes on HIV replication using integer-order modeling. The impact of memory effects on the molecular interaction model in HIV intracellular dynamics has not yet been thoroughly explored. In this work, we explore how physical interactions between RT and IN enzymes inhibit viral DNA production and PIC formation, employing enzyme-kinetic-based mathematical modeling enriched by fractional calculus and memory-based approaches.

Fractional mathematical models are gaining significant attention for real-world applications due to their ability to incorporate memory effects and capture crossover behavior in diverse physical contexts. In 1991, Westerlund proposed that all matter retains a memory, and past experiences impact its current behavior [11]. This principle has motivated the development of fractional models in various domains. Fractional calculus has been applied in tumor-immune modeling [12], infectious disease dynamics [13], environmental modeling [14], and physical systems like mass pendulum oscillations [15]. These diverse applications highlight the flexibility and biological relevance of fractional-order systems. Motivated by these successful applications, we utilize a fractional modeling framework to investigate HIV replication, where enzyme interactions, particularly between RT and IN, exhibit memory-dependent dynamics.

In HIV replication, the interaction between RT and IN involves complex biochemical and physical mechanisms influenced by memory effects, where past enzymatic states impact current activity. Specifically, integrase regulates RT via cis-allosteric interactions that alter RT's conformation and function during reverse transcription [16]. Classical integer-order models are limited in capturing such history-dependent dynamics. In contrast, fractional-order differential equations, particularly those using Caputo, Caputo-Fabrizio, and Atangana-Baleanu in the Caputo sense, enable accurate modeling of biological memory through distinct kernel structures. These operators capture short and long-term memory behaviors essential for representing enzyme regulation over time. Motivated by this, our study develops a fractional kinetic model to investigate how memory-driven RT-IN interactions shape the formation of the PIC, offering insights into potential targets for more effective antiretroviral therapy.

Integer-order (IO) derivatives focus only on local properties of a system at a specific time t. However, the question arises of how to account for the system's non-local behavior. Riemann and Liouville addressed this limitation by introducing fractional-order operators, which account for the broader, nonlocal interactions, offering a more comprehensive view of dynamic systems [17]. The concept of fractional derivatives, a generalization of integer-order derivatives, dates back to 1695 when L'Hospital asked Leibniz in a letter: 'What might be a derivative of order 1/2?' [18]. Since then, fractional calculus has progressed enormously and become an important field in mathematics and its applications in diverse areas such as biomathematics, disease dynamics, circuit design, fluid mechanics, nanofluid studies, social modeling, and dynamical systems analysis.

Kernel functions act as memory functions in fractional derivatives [19]. In this study, we

investigate the impact of three kernels, each uniquely modeling memory effects in the RT and IN enzyme interactions within the pre-integration complex. The power law-type kernel, introduced by Caputo in 1965 [20], emphasizes long-term memory. Later, in 2015, Caputo and Fabrizio presented a new definition known as the exponentially decaying type kernel [21], focusing on short-term dynamics characterized by exponential decay. Meanwhile, Atangana and Baleanu proposed the Mittag-Leffler kernel in 2016 [22], which balances both short and long-term memory effects on the system. This comprehensive strategy enables us to address the complexity of the physical and biochemical interactions between RT and IN enzymes, which inhibit each other in the pre-integration complex, enhancing our analysis and facilitating a deeper understanding of the underlying dynamics.

The primary objective of this study is to explore the intricate molecular interactions between RT and IN enzymes during the HIV replication process, with a specific focus on their physical and biochemical interactions. By incorporating fractional-order mathematical modeling with three distinct operators, Caputo, Caputo-Fabrizio, and Atangana-Baleanu in the Caputo sense, this study aims to illustrate the role of memory effects and past states in shaping these molecular dynamics. Through the integration of fractional calculus, the study provides a more realistic and complex representation of the biological system, capturing non-local and non-Markovian behaviors inherent in molecular interactions. Furthermore, global sensitivity analysis is employed to identify key reaction parameters critical to viral DNA synthesis and PIC formation. These findings enhance our understanding of HIV replication mechanisms and establish a robust interdisciplinary framework that bridges molecular biology and applied mathematics, informing future research in the field.

§2 Mathematical preliminaries

This section introduces some key fundamental definitions and theorems of fractional calculus essential for the analysis presented in this manuscript.

Definition 1. [20] The Caputo fractional derivative of order ζ is defined by

$$^{C}\mathcal{D}_t^{\zeta}[f(t)] = \frac{1}{\Gamma(n-\zeta)}\int_0^t (t-s)^{n-\zeta-1} f^{(n)}(s)ds.$$

Definition 2. [21] The Caputo-Fabrizio fractional derivative of order α is followed by

$$^{CF}\mathcal{D}_t^{\alpha}[f(t)] = \frac{M(\alpha)}{1-\alpha}\int_0^t f'(s)\exp\left[-\alpha\frac{t-s}{1-\alpha}\right]ds, t>0.$$

Where $M(\alpha)$ is the normalizing function corresponding to Caputo-Fabrizio differential operator defined by $M(\alpha)=\frac{2}{2-\alpha}$.

Definition 3. [22] Let $f(t)\in\mathcal{H}^1(0,T)$ where $T>0$, the Atangana-Baleanu operator in the Caputo sense of order $\sigma(\sigma\geq 0)$ is defined by,

$$^{\text{ABC}}\mathcal{D}_t^{\sigma}[f(t)] = \frac{\mathbf{B}(\sigma)}{1-\sigma}\int_0^t f'(s)\mathbf{E}_{\sigma}\left[-\frac{\sigma}{1-\sigma}(t-s)^{\sigma}\right]ds.$$

where $\mathbf{B}(\sigma)$ denotes the normalizing function of ABC method and defined by $\mathbf{B}(\sigma)=1-\sigma+\frac{\sigma}{\Gamma(\sigma)}$.

Definition 4. [22] The Atangana-Baleanu-Caputo integral operator of order $\sigma(\sigma \geq 0)$ is defined by

$$^{\mathrm{ABC}}I_t^{\sigma}[f(t)] = \frac{1-\sigma}{\mathbf{B}(\sigma)}f(t) + \frac{\sigma}{\mathbf{B}(\sigma)\Gamma(\sigma)}\int_0^t f(s)(t-s)^{\sigma-1}ds.$$

Definition 5. [23] The Sumudu transform of Atangana-Baleanu in the Caputo sense is as follows:

$$\mathbf{ST}\left\{^{\mathrm{ABC}}\mathcal{D}_t^{\sigma}[f(t)]\right\} = \frac{\mathbf{B}(\sigma)}{1-\sigma}\left(\sigma\left(\Gamma(\sigma)+1\right)E_{\sigma}\left(-\frac{1}{1-\sigma}u^{\sigma}\right)\right)\left(\mathbf{ST}(f(t)) - f(0)\right).$$

Theorem 2.1 (24)**.** *(Picard T stability theorem) Suppose* $\left(\mathbb{H}, \|.\|\right)$ *be a Banach space and T be the self map on* $\mathbb{H}$*, which satisfies the following*

$$\|T_x - T_y\| \leq G\|x - T_x\| + \mathcal{L}\|x - y\| \tag{1}$$

for all x,y $\in \mathbb{H}$ *where* $G \geq 0$ *and* $0 \leq \mathcal{L} < 1$*. Suppose T has a fixed point, then T is Picard's T-stable.*

§3 Mathematical modeling on molecular mechanism: Integer and fractional orders

Molecular studies enhance our understanding of the replication process and help in identifying specific therapeutic targets. Here, we introduce the fundamental ODE-based mathematical model developed by Ghosh et al. [10], which investigates the competitive relationship between the physical and biochemical interactions of HIV RT and IN enzymes, highlighting their roles in HIV-1 replication. These two molecular interactions (physical and biochemical) between RT and IN enzymes are depicted in the schematic Fig. 1. The Michaelis-Menten reaction scheme corresponding to the mathematical model as well as the schematic diagram as follows.

Michaelis Menten Reaction Scheme:

$$E_{RT} + \mathcal{S}_{RNA} \underset{K_{-1}}{\overset{K_1}{\rightleftharpoons}} C_1 \xrightarrow{K_2} \mathcal{S}_{vDNA} + E_{RT},$$
$$E_{IN} + \mathcal{S}_{vDNA} \underset{K_{-3}}{\overset{K_3}{\rightleftharpoons}} C_2,$$
$$E_{RT} + E_{IN} \underset{K_{-4}}{\overset{K_4}{\rightleftharpoons}} C_3.$$

The mathematical model corresponding to this reaction scheme is formulated using the law of mass action theory is as follows:

$$\begin{cases} \frac{dE_{RT}}{dt} = -K_1 E_{RT}\mathcal{S}_{RNA} + (K_{-1}+K_2)C_1 - K_4 E_{RT}E_{IN} + K_{-4}C_3, \\ \frac{d\mathcal{S}_{RNA}}{dt} = -K_1 E_{RT}\mathcal{S}_{RNA} + K_{-1}C_1, \\ \frac{dC_1}{dt} = K_1 E_{RT}\mathcal{S}_{RNA} - (K_{-1}+K_2)C_1, \\ \frac{d\mathcal{S}_{vDNA}}{dt} = K_2 C_1 - K_3 \mathcal{S}_{vDNA}E_{IN} + K_{-3}C_2, \\ \frac{dE_{IN}}{dt} = -K_3 \mathcal{S}_{vDNA}E_{IN} + K_{-3}C_2 - K_4 E_{RT}E_{IN} + K_{-4}C_3, \\ \frac{dC_2}{dt} = K_3 \mathcal{S}_{vDNA}E_{IN} - K_{-3}C_2, \\ \frac{dC_3}{dt} = K_4 E_{RT}E_{IN} - K_{-4}C_3, \end{cases} \tag{2}$$

with the initial conditions $E_{RT}(0) > 0$, $\mathcal{S}_{RNA}(0) > 0$, $E_{IN}(0) > 0$, $S_{vDNA}(0) = C_1(0) = C_2(0) = C_3(0) = 0$. Here E_{RT} and E_{IN} denote the concentrations of RT and IN enzymes, respectively. $\mathcal{S}_{RNA}$ and $\mathcal{S}_{vDNA}$ represent the single-stranded RNA and viral double-stranded DNA. C_1, C_2 and C_3 correspond to the concentrations of $RT-RNA$, $IN-vDNA$ and $RT-IN$ complexes, respectively. The parameters K_1 and K_{-1} represent the association and disassociation rate constant between RT enzyme and single-stranded RNA, respectively. K_2 describes the exposure rate of $RT-RNA$ complex (C_1). Similarly K_3 and K_{-3} denote the association and dissociation rate constants between IN enzyme and viral double-stranded DNA, respectively. The rate constants K_4 and K_{-4} represent the association and dissociation rate constants between the direct (physical) interaction between RT and IN enzymes, respectively. The definition of all rate constants is summarized in the Table 1.

Recently, fractional-order derivatives have significantly influenced the modeling of various biological phenomena [25, 26]. Fractional derivatives with nonsingular kernels have emerged as a powerful alternative to classical fractional operators that involve singular kernels. Unlike singular kernels that often involve power-law behaviors leading to strong singularities at the origin, nonsingular kernels are based on smooth functions such as exponential and Mittag-Leffler functions, providing better numerical stability and physical realism in modeling memory and hereditary properties of materials and processes. These nonsingular kernels are pivotal in applications requiring long-term memory effects without introducing mathematical singularities.

In this study, our objective is to explore the memory effect in the competitive interaction between RT and IN enzymes. To achieve this, we modify the basic integer-order model (2) by replacing the time derivative with three different kernel functions. However, in the fractional model, where the integer-order derivative is replaced by a fractional-order derivative, a crucial question arises regarding the model's dimensional imbalance. In the dimensional analysis of a model, directly substituting an integer-order derivative with a fractional-order derivative can be mathematically and biologically misleading in real-world scenarios.

To rectify this dimensional imbalance, we introduce a parameter L known as the memory rate parameter in the left-side of all fractional systems, with a dimension equivalent to $(hour)^{-1}$. The memory rate parameter in a time-fractional biological model is a powerful tool for representing how biological systems integrate and respond to past information. It provides insights into the

complexity of biological processes with memory and hereditary properties. Now, we present the three different fractional models, each corresponding to a different fractional operator, incorporating the memory rate parameter.

The Caputo fractional model, where the kernel is of the power-law type, is as follows:

(I) Caputo Fractional Model

$$\begin{cases} L^{(1-\zeta)}\ {}^{\mathrm{C}}D_t^{\zeta}E_{RT}(t) = -K_1E_{RT}\mathcal{S}_{RNA} + (K_{-1}+K_2)C_1 - K_4E_{RT}E_{IN} + K_{-4}C_3, \\ L^{(1-\zeta)}\ {}^{\mathrm{C}}D_t^{\zeta}\mathcal{S}_{RNA}(t) = -K_1E_{RT}\mathcal{S}_{RNA} + K_{-1}C_1, \\ L^{(1-\zeta)}\ {}^{\mathrm{C}}D_t^{\zeta}C_1(t) = -K_1E_{RT}\mathcal{S}_{RNA} - (K_{-1}+K_2)C_1, \\ L^{(1-\zeta)}\ {}^{\mathrm{C}}D_t^{\zeta}\mathcal{S}_{vDNA}(t) = K_2C_1 - K_3\mathcal{S}_{vDNA}E_{IN} + K_{-3}C_2, \\ L^{(1-\zeta)}\ {}^{\mathrm{C}}D_t^{\zeta}E_{IN}(t) = -K_3\mathcal{S}_{vDNA}E_{IN} + K_{-3}C_2 - K_4E_{RT}E_{IN} + K_{-4}C_3, \\ L^{(1-\zeta)}\ {}^{\mathrm{C}}D_t^{\zeta}C_2(t) = K_3\mathcal{S}_{vDNA}E_{IN} - K_{-3}C_2, \\ L^{(1-\zeta)}\ {}^{\mathrm{C}}D_t^{\zeta}C_3(t) = K_4E_{RT}E_{IN} - K_{-4}C_3, \end{cases} \tag{3}$$

with the initial conditions as same as the integer order system (2). Here $\zeta \in (0,1]$ is the fractional order of the derivative as the index of memory for this Caputo system. Now the Caputo-Fabrizio fractional system where the kernel is exponentially decaying type is as follows:

(II) Caputo-Fabrizio Fractional Model

$$\begin{cases} L^{(1-\alpha)}\ {}^{\mathrm{CF}}D_t^{\alpha}E_{RT}(t) = -K_1E_{RT}\mathcal{S}_{RNA} + (K_{-1}+K_2)C_1 - K_4E_{RT}E_{IN} + K_{-4}C_3, \\ L^{(1-\alpha)}\ {}^{\mathrm{CF}}D_t^{\alpha}\mathcal{S}_{RNA}(t) = -K_1E_{RT}\mathcal{S}_{RNA} + K_{-1}C_1, \\ L^{(1-\alpha)}\ {}^{\mathrm{CF}}D_t^{\alpha}C_1(t) = -K_1E_{RT}\mathcal{S}_{RNA} - (K_{-1}+K_2)C_1, \\ L^{(1-\alpha)}\ {}^{\mathrm{CF}}D_t^{\alpha}\mathcal{S}_{vDNA}(t) = K_2C_1 - K_3\mathcal{S}_{vDNA}E_{IN} + K_{-3}C_2, \\ L^{(1-\alpha)}\ {}^{\mathrm{CF}}D_t^{\alpha}E_{IN}(t) = -K_3\mathcal{S}_{vDNA}E_{IN} + K_{-3}C_2 - K_4E_{RT}E_{IN} + K_{-4}C_3, \\ L^{(1-\alpha)}\ {}^{\mathrm{CF}}D_t^{\alpha}C_2(t) = K_3\mathcal{S}_{vDNA}E_{IN} - K_{-3}C_2, \\ L^{(1-\alpha)}\ {}^{\mathrm{CF}}D_t^{\alpha}C_3(t) = K_4E_{RT}E_{IN} - K_{-4}C_3, \end{cases} \tag{4}$$

with the same initial conditions as the integer order system (2) and $\alpha \in (0,1]$ represent fractional order of derivative as index of memory of this Caputo-Fabrizio system. Finally the system with Mittag-Leffler kernel known as ABC fractional order model is as follows:

(III) Fractional Model of Atangana-Baleanu in the Caputo Sense

$$\begin{cases} L^{(1-\sigma)}\ {}^{\mathrm{ABC}}D_t^{\sigma}E_{RT}(t) = -K_1E_{RT}\mathcal{S}_{RNA} + (K_{-1}+K_2)C_1 - K_4E_{RT}E_{IN} + K_{-4}C_3, \\ L^{(1-\sigma)}\ {}^{\mathrm{ABC}}D_t^{\sigma}\mathcal{S}_{RNA}(t) = -K_1E_{RT}\mathcal{S}_{RNA} + K_{-1}C_1, \\ L^{(1-\sigma)}\ {}^{\mathrm{ABC}}D_t^{\sigma}C_1(t) = -K_1E_{RT}\mathcal{S}_{RNA} - (K_{-1}+K_2)C_1, \\ L^{(1-\sigma)}\ {}^{\mathrm{ABC}}D_t^{\sigma}\mathcal{S}_{vDNA}(t) = K_2C_1 - K_3\mathcal{S}_{vDNA}E_{IN} + K_{-3}C_2, \\ L^{(1-\sigma)}\ {}^{\mathrm{ABC}}D_t^{\sigma}E_{IN}(t) = -K_3\mathcal{S}_{vDNA}E_{IN} + K_{-3}C_2 - K_4E_{RT}E_{IN} + K_{-4}C_3, \\ L^{(1-\sigma)}\ {}^{\mathrm{ABC}}D_t^{\sigma}C_2(t) = K_3\mathcal{S}_{vDNA}E_{IN} - K_{-3}C_2, \\ L^{(1-\sigma)}\ {}^{\mathrm{ABC}}D_t^{\sigma}C_3(t) = K_4E_{RT}E_{IN} - K_{-4}C_3, \end{cases} \tag{5}$$

with the initial conditions as the integer order model (2). The memory index $\sigma \in (0,1])$ denotes the fractional order of the derivative of this ABC system.

Table 1. Description of all the kinetic parameters and the specified ranges of values used in the numerical simulations. Sources of all parameters are given in detail in the table.

Parameter	Definition	Range ($hour^{-1}$)	Reference
K_1	Forward rate constant for the formation of RT-RNA complex C_1	0.5-1.5 $(\mu mol/l)^{-1}$	[10, 27]
K_2	Rate constant of vDNA formation from C_1 complex	0.1-0.7	[9, 10, 28]
K_3	Forward rate constant for the formation of IN-DNA complex C_2	0.5-1.5 $(\mu mol/l)^{-1}$	[9, 10]
K_4	Forward rate constant for the formation of RT-IN complex C_3	0.5-3.0 $(\mu mol/l)^{-1}$	[9, 10]
K_{-1}	Rate constant for the backward reaction of complex C_1	0.01-0.1	[10, 27]
K_{-3}	Rate constant for the backward reaction of complex C_3	0.01-0.1	[9, 10]
K_{-4}	Rate constant for the backward reaction of complex C_4	0.01-0.1	[9, 10]

§4 Mathematical validation of molecular reaction dynamics: Existence and uniqueness

The existence and uniqueness of solutions in a fractional model are essential for accurately predicting viral behavior within a biological context. These properties also help the development of stable numerical methods and provide deep insights into system dynamics. Now we will prove the uniqueness and existence of the solution of our proposed fractional-order mathematical model using fixed point theory considering the Atangana-Baleanu fractional operator in the Caputo sense (ABC).

Applying the definition (4) of the ABC fractional integral operator on both sides of system (5), we obtain

$$\begin{cases} E_{RT}(t) - E_{RT}(0) = L^{(\sigma-1)\ ABC}\boldsymbol{I}^{\sigma}_{0,t}(-K_1E_{RT}\mathcal{S}_{RNA} + (K_{-1}+K_2)C_1 - K_4E_{RT}E_{IN} \\ \qquad\qquad +K_{-4}C_3), \\ \mathcal{S}_{RNA}(t) - \mathcal{S}_{RNA}(0) = L^{(\sigma-1)\ ABC}\boldsymbol{I}^{\sigma}_{0,t}(-K_1E_{RT}\mathcal{S}_{RNA} + K_{-1}C_1), \\ C_1(t) - C_1(0) = L^{(\sigma-1)\ ABC}\boldsymbol{I}^{\sigma}_{0,t}(K_1E_{RT}\mathcal{S}_{RNA} - (K_{-1}+K_2)C_1), \\ \mathcal{S}_{vDNA}(t) - \mathcal{S}_{vDNA}(0) = L^{(\sigma-1)\ ABC}\boldsymbol{I}^{\sigma}_{0,t}(K_2C_1 - K_3\mathcal{S}_{vDNA}E_{IN} + K_{-3}C_2), \\ E_{IN}(t) - E_{IN}(0) = L^{(\sigma-1)\ ABC}\boldsymbol{I}^{\sigma}_{0,t}(-K_3\mathcal{S}_{vDNA}E_{IN} + K_{-3}C_2 - K_4E_{RT}E_{IN} + K_{-4}C_3), \\ C_2(t) - C_2(0) = L^{(\sigma-1)\ ABC}\boldsymbol{I}^{\sigma}_{0,t}(K_3\mathcal{S}_{vDNA}E_{IN} - K_{-3}C_2), \\ C_3(t) - C_3(0) = L^{(\sigma-1)\ ABC}\boldsymbol{I}^{\sigma}_{0,t}(K_4E_{RT}E_{IN} - K_{-4}C_3). \end{cases} \tag{6}$$

This implies that

$$\begin{cases} E_{RT}(t) - E_{RT}(0) = \frac{L^{(\sigma-1)}(1-\sigma)}{\mathbf{B}(\sigma)}\mathcal{J}_1(E_{RT}(t),t) + \frac{L^{(\sigma-1)}\sigma}{\mathbf{B}(\sigma)\Gamma(\sigma)} \times \int_0^t (t-\xi)^{\sigma-1}\mathcal{J}_1(E_{RT}(\xi),\xi)d\xi, \\ \mathcal{S}_{RNA}(t) - \mathcal{S}_{RNA}(0) = \frac{L^{(\sigma-1)}(1-\sigma)}{\mathbf{B}(\sigma)}\mathcal{J}_2(\mathcal{S}_{RNA}(t),t) + \frac{L^{(\sigma-1)}\sigma}{\mathbf{B}(\sigma)\Gamma(\sigma)} \\ \qquad\qquad \times \int_0^t (t-\xi)^{\sigma-1}\mathcal{J}_2(\mathcal{S}_{RNA}(\xi),\xi)d\xi, \end{cases}$$

$$\begin{cases} \mathcal{S}_{vDNA}(t)-\mathcal{S}_{vDNA}(0)=\frac{L^{(\sigma-1)}(1-\sigma)}{\mathbf{B}(\sigma)}\mathcal{J}_4(\mathcal{S}_{vDNA}(t),t)+\frac{L^{(\sigma-1)}\sigma}{\mathbf{B}(\sigma)\Gamma(\sigma)} \\ \qquad\qquad \times\int_0^t(t-\xi)^{\sigma-1}\mathcal{J}_4(\mathcal{S}_{vDNA}(\xi),\xi)d\xi, \\ E_{IN}(t)-E_{IN}(0)=\frac{L^{(\sigma-1)}(1-\sigma)}{\mathbf{B}(\sigma)}\mathcal{J}_5(E_{RT}(t),t)+\frac{L^{(\sigma-1)}\sigma}{\mathbf{B}(\sigma)\Gamma(\sigma)}\times\int_0^t(t-\xi)^{\sigma-1}\mathcal{J}_5(E_{IN}(\xi),\xi)d\xi, \\ C_2(t)-C_2(0)=\frac{L^{(\sigma-1)}(1-\sigma)}{\mathbf{B}(\sigma)}\mathcal{J}_6(C_2(t),t)+\frac{L^{(\sigma-1)}\sigma}{\mathbf{B}(\sigma)\Gamma(\sigma)}\times\int_0^t(t-\xi)^{\sigma-1}\mathcal{J}_6(C_2(\xi),\xi)d\xi, \\ C_3(t)-C_3(0)=\frac{L^{(\sigma-1)}(1-\sigma)}{\mathbf{B}(\sigma)}\mathcal{J}_7(C_3(t),t)+\frac{L^{(\sigma-1)}\sigma}{\mathbf{B}(\sigma)\Gamma(\sigma)}\times\int_0^t(t-\xi)^{\sigma-1}\mathcal{J}_7(C_3(\xi),\xi)d\xi. \end{cases} \tag{7}$$

The kernels $\mathcal{J}_1(E_{RT}(t),t)$, $\mathcal{J}_2(\mathcal{S}_{RNA}(t),t)$, $\mathcal{J}_3(C_1(t),t)$, $\mathcal{J}_4(\mathcal{S}_{vDNA}(t),t)$, $\mathcal{J}_5(E_{IN}(t),t)$, $\mathcal{J}_6(C_2(t),t)$ and $\mathcal{J}_7(C_3(t),t)$ are as follows:

$$\begin{cases} \mathcal{J}_1(E_{RT}(t),t)=-K_1E_{RT}\mathcal{S}_{RNA}+(K_{-1}+K_2)C_1-K_4E_{RT}E_{IN}+K_{-4}C_3, \\ \mathcal{J}_2(\mathcal{S}_{RNA}(t),t)=-K_1E_{RT}\mathcal{S}_{RNA}+K_{-1}C_1, \\ \mathcal{J}_3(C_1(t),t)=K_1E_{RT}\mathcal{S}_{RNA}-(K_{-1}+K_2)C_1, \\ \mathcal{J}_4(\mathcal{S}_{vDNA}(t),t)=K_2C_1-K_3\mathcal{S}_{vDNA}E_{IN}+K_{-3}C_2, \\ \mathcal{J}_5(E_{IN}(t),t)=-K_3\mathcal{S}_{vDNA}E_{IN}+K_{-3}C_2-K_4E_{RT}E_{IN}+K_{-4}C_3, \\ \mathcal{J}_6(C_2(t),t)=K_3\mathcal{S}_{vDNA}E_{IN}-K_{-3}C_2, \\ \mathcal{J}_7(C_3(t),t)=K_4E_{RT}E_{IN}-K_{-4}C_3. \end{cases}$$

Now we prove that the kernels $\mathcal{J}_1$, $\mathcal{J}_2$, $\mathcal{J}_3$, $\mathcal{J}_4$, $\mathcal{J}_5$, $\mathcal{J}_6$ and $\mathcal{J}_7$ satisfy the Lipchitz condition under some assumption. Let the entire population of our system have an upper bound. Then there exist some positive real numbers $\mathcal{U}_1$, $\mathcal{U}_2$, $\mathcal{U}_3$, $\mathcal{U}_4$, $\mathcal{U}_5$, $\mathcal{U}_6$ and $\mathcal{U}_7$ such that $\|E_{RT}\|\le\mathcal{U}_1$, $\|\mathcal{S}_{RNA}\|\le\mathcal{U}_2$, $\|C_1\|\le\mathcal{U}_3$, $\|\mathcal{S}_{vDNA}\|\le\mathcal{U}_4$, $\|E_{IN}\|\le\mathcal{U}_5$, $\|C_2\|\le\mathcal{U}_6$, and $\|C_3\|\le\mathcal{U}_7$.

First, we prove for the kernel $\mathcal{J}_1$ and can follow the same approach for other kernels. Let E_{RT} and E_{RT_1} are two functions, then using the property of the norm function we have

$$\begin{aligned} &\|\mathcal{J}_1(E_{RT}(t),t)-\mathcal{J}_1\left(E_{RT_1}(t),t\right)\| \\ =&\|-K_1\mathcal{S}_{RNA}(t)\left(E_{RT}(t)-E_{RT_1}(t)\right)-K_4E_{IN}(t)\left(E_{RT}(t)-E_{RT_1}(t)\right)\| \\ \le&(K_1\mathcal{U}_2+K_4\mathcal{U}_5)\left\|E_{RT}(t)-E_{RT_1}(t)\right\|. \end{aligned}$$

Considering $\mathcal{V}_1=((\mathcal{K}_1\mathcal{U}_2+K_4\mathcal{U}_5)$, we obtain

$$\|\mathcal{J}_1(E_{RT}(t),t)-\mathcal{J}_1\left(E_{RT_1}(t),t\right)\|\le\mathcal{V}_1\left\|E_{RT}(t)-E_{RT_1}(t)\right\|.$$

In a similar manner, the Lipschitz condition for the other kernels can be verified as follows:

$$\begin{cases} \|\mathcal{J}_2(\mathcal{S}_{RNA}(t),t)-\mathcal{J}_2\left(\mathcal{S}_{RNA_1}(t),t\right)\|\le\mathcal{V}_2\left\|\mathcal{S}_{RNA}(t)-\mathcal{S}_{RNA_1}(t)\right\|, \\ \|\mathcal{J}_3(C_1(t),t)-\mathcal{J}_3\left(C_{1_1}(t),t\right)\|\le\mathcal{V}_3\left\|C_1(t)-C_{1_1}(t)\right\|, \\ \|\mathcal{J}_4(\mathcal{S}_{vDNA}(t),t)-\mathcal{J}_4\left(\mathcal{S}_{vDNA_1}(t),t\right)\|\le\mathcal{V}_4\left\|\mathcal{S}_{vDNA}(t)-\mathcal{S}_{vDNA_1}(t)\right\|, \\ \|\mathcal{J}_5(E_{IN}(t),t)-\mathcal{J}_5\left(E_{IN_1}(t),t\right)\|\le\mathcal{V}_5\left\|E_{IN}(t)-E_{IN_1}(t)\right\|, \\ \|\mathcal{J}_6(C_2(t),t)-\mathcal{J}_6\left(C_{2_1}(t),t\right)\|\le\mathcal{V}_6\left\|C_2(t)-C_{2_1}(t)\right\|, \\ \|\mathcal{J}_7(C_3(t),t)-\mathcal{J}_7\left(C_{3_1}(t),t\right)\|\le\mathcal{V}_7\left\|C_3(t)-C_{3_1}(t)\right\|. \end{cases}$$

Taking the recursive relation in the expression (7), we get

$$\begin{cases} E_{RT_n}(t) = \frac{L^{(\sigma-1)}(1-\sigma)}{\mathbf{B}(\sigma)}\mathcal{J}_1(E_{RT_{n-1}}(t),t) + \frac{L^{(\sigma-1)}\sigma}{\mathbf{B}(\sigma)\Gamma(\sigma)} \times \int_0^t (t-\xi)^{\sigma-1}\mathcal{J}_1(E_{RT_{n-1}}(\xi),\xi)d\xi \\ \qquad +E_{RT}(0), \\ \mathcal{S}_{RNA_n}(t) = \frac{L^{(\sigma-1)}(1-\sigma)}{\mathbf{B}(\sigma)}\mathcal{J}_2(\mathcal{S}_{RNA_{n-1}}(t),t) + \frac{L^{(\sigma-1)}\sigma}{\mathbf{B}(\sigma)\Gamma(\sigma)} \times \int_0^t (t-\xi)^{\sigma-1}\mathcal{J}_2(\mathcal{S}_{RNA_{n-1}}(\xi),\xi)d\xi \\ \qquad +\mathcal{S}_{RNA}(0), \\ C_{1_n}(t) = \frac{L^{(\sigma-1)}(1-\sigma)}{\mathbf{B}(\sigma)}\mathcal{J}_3(C_{1_{n-1}}(t),t) + \frac{L^{(\sigma-1)}\sigma}{\mathbf{B}(\sigma)\Gamma(\sigma)} \times \int_0^t (t-\xi)^{\sigma-1}\mathcal{J}_3(C_{1_{n-1}}(\xi),\xi)d\xi + C_1(0), \\ \mathcal{S}_{vDNA_n}(t) = \frac{L^{(\sigma-1)}(1-\sigma)}{\mathbf{B}(\sigma)}\mathcal{J}_4(\mathcal{S}_{vDNA_{n-1}}(t),t) + \frac{L^{(\sigma-1)}\sigma}{\mathbf{B}(\sigma)\Gamma(\sigma)} \times \int_0^t (t-\xi)^{\sigma-1}\mathcal{J}_4(\mathcal{S}_{vDNA_{n-1}}(\xi),\xi)d\xi \\ \qquad +\mathcal{S}_{vDNA}(0), \\ E_{IN_n}(t) = \frac{L^{(\sigma-1)}(1-\sigma)}{\mathbf{B}(\sigma)}\mathcal{J}_5(E_{IN_{n-1}}(t),t) + \frac{L^{(\sigma-1)}\sigma}{\mathbf{B}(\sigma)\Gamma(\sigma)} \times \int_0^t (t-\xi)^{\sigma-1}\mathcal{J}_5(E_{IN_{n-1}}(\xi),\xi)d\xi \\ \qquad +E_{IN}(0), \\ C_{2_n}(t) = \frac{L^{(\sigma-1)}(1-\sigma)}{\mathbf{B}(\sigma)}\mathcal{J}_6(C_{2_{n-1}}(t),t) + \frac{L^{(\sigma-1)}\sigma}{\mathbf{B}(\sigma)\Gamma(\sigma)} \times \int_0^t (t-\xi)^{\sigma-1}\mathcal{J}_6(C_{2_{n-1}}(\xi),\xi)d\xi + C_2(0), \\ C_{3_n}(t) = \frac{L^{(\sigma-1)}(1-\sigma)}{\mathbf{B}(\sigma)}\mathcal{J}_7(C_{3_{n-1}}(t),t) + \frac{L^{(\sigma-1)}\sigma}{\mathbf{B}(\sigma)\Gamma(\sigma)} \times \int_0^t (t-\xi)^{\sigma-1}\mathcal{J}_7(C_{3_{n-1}}(\xi),\xi)d\xi + C_3(0), \end{cases} \tag{8}$$

along with the initial conditions as same as the system (2). Now we take the difference between the successive terms to have

$$\begin{cases} \Phi_{1n}(t) = \quad E_{RT_n}(t) - E_{RT_{n-1}}(t) = \frac{L^{(\sigma-1)}(1-\sigma)}{\mathbf{B}(\sigma)}\left(\mathcal{J}_1\left(E_{RT_{n-1}}(t),t\right) - \mathcal{J}_1\left(E_{RT_{n-2}}(t),t\right)\right) \\ \qquad +\frac{L^{(\sigma-1)}\sigma}{\mathbf{B}(\sigma)\Gamma(\sigma)}\int_0^t (t-\xi)^{\sigma-1}\left(\mathcal{J}_1\left(E_{RT_{n-1}}(\xi),\xi\right) - \mathcal{J}_1\left(E_{RT_{n-2}}(\xi),\xi\right)\right)d\xi, \\ \Phi_{2n}(t) = \quad \mathcal{S}_{RNA_n}(t) - \mathcal{S}_{RNA_{n-1}}(t) = \frac{L^{(\sigma-1)}(1-\sigma)}{\mathbf{B}(\sigma)}\left(\mathcal{J}_2\left(\mathcal{S}_{RNA_{n-1}}(t),t\right) - \mathcal{J}_2\left(\mathcal{S}_{RNA_{n-2}}(t),t\right)\right) \\ \qquad +\frac{L^{(\sigma-1)}\sigma}{\mathbf{B}(\sigma)\Gamma(\sigma)}\int_0^t (t-\xi)^{\sigma-1}\left(\mathcal{J}_2\left(\mathcal{S}_{RNA_{n-1}}(\xi),\xi\right) - \mathcal{J}_2\left(\mathcal{S}_{RNA_{n-2}}(\xi),\xi\right)\right)d\xi, \\ \Phi_{3n}(t) = \quad C_{1_n}(t) - C_{1_{n-1}}(t) = \frac{L^{(\sigma-1)}(1-\sigma)}{\mathbf{B}(\sigma)}\left(\mathcal{J}_3\left(C_{1_{n-1}}(t),t\right) - \mathcal{J}_3\left(C_{1_{n-2}}(t),t\right)\right) \\ \qquad +\frac{L^{(\sigma-1)}\sigma}{\mathbf{B}(\sigma)\Gamma(\sigma)}\int_0^t (t-\xi)^{\sigma-1}\left(\mathcal{J}_3\left(C_{1_{n-1}}(\xi),\xi\right) - \mathcal{J}_3\left(C_{2_{n-2}}(\xi),\xi\right)\right)d\xi, \\ \Phi_{4n}(t) = \quad \mathcal{S}_{vDNA_n}(t) - \mathcal{S}_{vDNA_{n-1}}(t) = \\ \qquad \frac{L^{(\sigma-1)}(1-\sigma)}{\mathbf{B}(\sigma)}\left(\mathcal{J}_4\left(\mathcal{S}_{vDNA_{n-1}}(t),t\right) - \mathcal{J}_4\left(\mathcal{S}_{vDNA_{n-2}}(t),t\right)\right) \\ \qquad +\frac{L^{(\sigma-1)}\sigma}{\mathbf{B}(\sigma)\Gamma(\sigma)}\int_0^t (t-\xi)^{\sigma-1}\left(\mathcal{J}_4\left(\mathcal{S}_{vDNA_{n-1}}(\xi),\xi\right) - \mathcal{J}_4\left(\mathcal{S}_{vDNA_{n-2}}(\xi),\xi\right)\right)d\xi, \\ \Phi_{5n}(t) = \quad E_{IN_n}(t) - E_{IN_{n-1}}(t) = \frac{L^{(\sigma-1)}(1-\sigma)}{\mathbf{B}(\sigma)}\left(\mathcal{J}_5\left(E_{IN_{n-1}}(t),t\right) - \left(\mathcal{J}_5\left(E_{IN_{n-2}}(t),t\right)\right)\right) \\ \qquad +\frac{L^{(\sigma-1)}\sigma}{\mathbf{B}(\sigma)\Gamma(\sigma)}\int_0^t (t-\xi)^{\sigma-1}\left(\mathcal{J}_5\left(E_{IN_{n-1}}(\xi),\xi\right) - \mathcal{J}_5\left(E_{IN_{n-2}}(\xi),\xi\right)\right)d\xi, \\ \Phi_{6n}(t) = \quad C_{2_n}(t) - C_{2_{n-1}}(t) = \frac{L^{(\sigma-1)}(1-\sigma)}{\mathbf{B}(\sigma)}\left(\mathcal{J}_6\left(C_{2_{n-1}}(t),t\right) - \mathcal{J}_6\left(C_{2_{n-2}}(t),t\right)\right) \\ \qquad +\frac{L^{(\sigma-1)}\sigma}{\mathbf{B}(\sigma)\Gamma(\sigma)}\int_0^t (t-\xi)^{\sigma-1}\left(\mathcal{J}_6\left(C_{2_{n-1}}(y),y\right) - \mathcal{J}_6\left(C_{2_{n-2}}(\xi),\xi\right)\right)d\xi, \\ \Phi_{7n}(t) = \quad C_{3_n}(t) - C_{3_{n-1}}(t) = \frac{L^{(\sigma-1)}(1-\sigma)}{\mathbf{B}(\sigma)}\left(\mathcal{J}_7\left(C_{3_{n-1}}(t),t\right) - \mathcal{J}_7\left(C_{3_{n-2}}(t),t\right)\right) \\ \qquad +\frac{L^{(\sigma-1)}\sigma}{\mathbf{B}(\sigma)\Gamma(\sigma)}\int_0^t (t-\xi)^{\sigma-1}\left(\mathcal{J}_7\left(C_{3_{n-1}}(\xi),\xi\right) - \mathcal{J}_7\left(C_{3_{n-2}}(\xi),\xi\right)\right)d\xi. \end{cases} \tag{9}$$

Taking norm of the first equation of the equation (9) and applying triangular inequality, we obtain

$$\|\Phi_{1n}(t)\| = \|E_{RT_n}(t) - E_{RT_{n-1}}(t)\|$$

$$
\begin{aligned}
&= \Big\| \frac{L^{(\sigma-1)}(1-\sigma)}{\mathbf{B}(\sigma)} \Big(\mathcal{J}_1(E_{RT_{n-1}}(t),t) - \mathcal{J}_1(E_{RT_{n-2}}(t),t) \Big) \\
&\quad + \frac{L^{(\sigma-1)}\sigma}{\mathbf{B}(\sigma)\Gamma(\sigma)} \int_0^t (t-\xi)^{\sigma-1} \Big(\mathcal{J}_1(E_{RT_{n-1}}(\xi),\xi) - \mathcal{J}_1(E_{RT_{n-2}}(\xi),\xi) \Big) d\xi \Big\| \\
&\leq \frac{L^{(\sigma-1)}(1-\sigma)}{\mathbf{B}(\sigma)} \big\| \mathcal{J}_1(E_{RT_{n-1}}(t),t) - \mathcal{J}_1(E_{RT_{n-2}}(t),t) \big\| \\
&\quad + \frac{L^{(\sigma-1)}\sigma}{\mathbf{B}(\sigma)\Gamma(\sigma)} \Big\| \int_0^t (t-\xi)^{\sigma-1} \Big(\mathcal{J}_1(E_{RT_{n-1}}(\xi),\xi) - \mathcal{J}_1(E_{RT_{n-2}}(\xi),\xi) \Big) d\xi \Big\|. \qquad (10)
\end{aligned}
$$

Theorem 4.1. *The fractional system (5) has a unique solution for $t \in [0,T]$ if the following conditions are satisfied*

$$
\left(\frac{1-\sigma}{\mathbf{B}(\sigma)} \mathcal{V}_i + \frac{T^\sigma}{\mathbf{B}(\sigma)\Gamma(\sigma)} \mathcal{V}_i \right)^n < 1, \quad i = 1,2,...,7. \qquad (11)
$$

Proof. Since all population of our system is bounded and the kernels $\mathcal{J}_i,\ i = 1,2,...,7$ are satisfied the Lipschitz condition. Thus applying these properties of all kernels along with recursive principle on the equation (10), we obtain

$$
\begin{aligned}
\|\Phi_{1n}(t)\| &\leq \left(\frac{L^{(\sigma-1)}(1-\sigma)}{\mathbf{B}(\sigma)} \right) \mathcal{V}_1 \|E_{RT_{n-1}}(t) - E_{RT_{n-2}}(t)\| + \left(\frac{L^{(\sigma-1)}\sigma}{\mathbf{B}(\sigma)\Gamma(\sigma)} \right) \mathcal{V}_1 \int_0^t \|E_{RT_{n-1}}(\xi) \\
&\quad - \quad E_{RT_{n-1}}(\xi)\| d\xi, \\
&= \left(\frac{L^{(\sigma-1)}(1-\sigma)}{\mathbf{B}(\sigma)} \right) \mathcal{V}_1 \|\Phi_{1(n-1)}(t)\| + \left(\frac{L^{(\sigma-1)}\sigma}{\mathbf{B}(\sigma)\Gamma(\sigma)} \right) \mathcal{V}_1 \int_0^t \|\Phi_{1(n-1)}(\xi)\| d\xi \\
&\leq \|E_{RT_0}(t)\| \left(\frac{L^{(\sigma-1)}(1-\sigma)}{\mathbf{B}(\sigma)} \mathcal{V}_1 + \frac{L^{(\sigma-1)}T^\sigma}{\mathbf{B}(\sigma)\Gamma(\sigma)} \mathcal{V}_1 \right)^n.
\end{aligned} \qquad (12)
$$

Similarly using all these properties of kernels on the equation (9) for the other population of our system, we have

$$
\begin{cases}
\|\Phi_{2n}(t)\| \leq \|\mathcal{S}_{RNA_0}(t)\| \left(\frac{L^{(\sigma-1)}(1-\sigma)}{\mathbf{B}(\sigma)} \mathcal{V}_2 + \frac{L^{(\sigma-1)}T^\sigma}{\mathbf{B}(\sigma)\Gamma(\sigma)} \mathcal{V}_2 \right)^n, \\
\|\Phi_{3n}(t)\| \leq \|C_{1_0}(t)\| \left(\frac{L^{(\sigma-1)}(1-\sigma)}{\mathbf{B}(\sigma)} \mathcal{V}_3 + \frac{L^{(\sigma-1)}T^\sigma}{\mathbf{B}(\sigma)\Gamma(\sigma)} \mathcal{V}_3 \right)^n, \\
\|\Phi_{4n}(t)\| \leq \|\mathcal{S}_{vDNA_0}(t)\| \left(\frac{L^{(\sigma-1)}(1-\sigma)}{\mathbf{B}(\sigma)} \mathcal{V}_4 + \frac{L^{(\sigma-1)}T^\sigma}{\mathbf{B}(\sigma)\Gamma(\sigma)} \mathcal{V}_4 \right)^n, \\
\|\Phi_{5n}(t)\| \leq \|E_{IN_0}(t)\| \left(\frac{L^{(\sigma-1)}(1-\sigma)}{\mathbf{B}(\sigma)} \mathcal{V}_5 + \frac{L^{(\sigma-1)}T^\sigma}{\mathbf{B}(\sigma)\Gamma(\sigma)} \mathcal{V}_5 \right)^n, \\
\|\Phi_{6n}(t)\| \leq \|C_{2_0}(t)\| \left(\frac{L^{(\sigma-1)}(1-\sigma)}{\mathbf{B}(\sigma)} \mathcal{V}_6 + \frac{L^{(\sigma-1)}T^\sigma}{\mathbf{B}(\sigma)\Gamma(\sigma)} \mathcal{V}_6 \right)^n, \\
\|\Phi_{7n}(t)\| \leq \|C_{3_0}(t)\| \left(\frac{L^{(\sigma-1)}(1-\sigma)}{\mathbf{B}(\sigma)} \mathcal{V}_7 + \frac{L^{(\sigma-1)}T^\sigma}{\mathbf{B}(\sigma)\Gamma(\sigma)} \mathcal{V}_7 \right)^n.
\end{cases} \qquad (13)
$$

Therefore the sequences described above exist and satisfy $\|\Phi_{1n}(t)\| \to 0$, $\|\Phi_{2n}(t)\| \to 0$, $\|\Phi_{3n}(t)\| \to 0$, $\|\Phi_{4n}(t)\| \to 0$, $\|\Phi_{5n}(t)\| \to 0$, $\|\Phi_{6n}(t)\| \to 0$ and $\|\Phi_{7n}(t)\| \to 0$ as $n \to \infty$ because

$$
\left(\frac{L^{(\sigma-1)}(1-\sigma)}{\mathbf{B}(\sigma)} \mathcal{V}_i + \frac{L^{(\sigma-1)}T^\sigma}{\mathbf{B}(\sigma)\Gamma(\sigma)} \mathcal{V}_i \right)^n < 1,
$$

by assertion. Furthermore, by applying the triangle inequality for any k, we obtain

$$\begin{cases} \left\| E_{RT_{n+p}} - E_{RT_n} \right\| \leq \sum_{i=n+1}^{n+p} M_1^i = \frac{M_1^{n+1} - M_1^{n+p+1}}{1-M_1}, \\ \left\| \mathcal{S}_{RNA_{n+p}}(t) - \mathcal{S}_{RNA_n}(t) \right\| \leq \sum_{i=n+1}^{n+p} M_2^i = \frac{M_2^{n+1} - M_2^{n+p+1}}{1-M_2}, \\ \left\| C_{1_{n+p}}(t) - C_{1_n}(t) \right\| \leq \sum_{i=n+1}^{n+p} M_3^i = \frac{M_3^{n+1} - M_3^{n+p+1}}{1-M_3}, \\ \left\| \mathcal{S}_{vDNA_{n+p}}(t) - \mathcal{S}_{vDNA_n}(t) \right\| \leq \sum_{i=n+1}^{n+p} M_4^i = \frac{M_4^{n+1} - M_4^{n+p+1}}{1-M_4}, \\ \left\| E_{IN_{n+p}} - E_{IN_n} \right\| \leq \sum_{i=n+1}^{n+p} M_5^i = \frac{M_5^{n+1} - M_5^{n+p+1}}{1-M_5}, \\ \left\| C_{2_{n+p}}(t) - C_{2_n}(t) \right\| \leq \sum_{i=n+1}^{n+p} M_6^i = \frac{M_6^{n+1} - M_6^{n+p+1}}{1-M_6}, \\ \left\| C_{3_{n+p}}(t) - C_{3_n}(t) \right\| \leq \sum_{i=n+1}^{n+p} M_7^i = \frac{M_7^{n+1} - M_7^{n+p+1}}{1-M_7}, \end{cases} \tag{14}$$

where $M_i,\ i = 1, 2, ..., 7$ are the expressions in the bracket on the right-side of the equation (13) within the parenthesis. Therefore the sequences $E_{RT_n}, \mathcal{S}_{RNA_n}, C_{1_n}, \mathcal{S}_{vDNA_n}, E_{IN_n}, C_{2_n}$ and C_{3_n} are regarded as a Cauchy sequences and they are uniformly convergent as result in [29].

Remark: The mathematical analysis of uniqueness ensures that the model yields a single biologically meaningful trajectory for given initial conditions and parameters. This is critical in the context of biochemical interactions, where the reproducibility of molecular responses is essential for accurate prediction and intervention strategies. Establishing uniqueness reinforces the reliability of the model to describe consistent behavior of RT and IN interactions during HIV replication.

§5 Stability insights in fractional molecular interaction model

In this section, we present Picard F-stability of all solutions for our system (5) utilizing the Sumudu transformation. Picard stability provides a rigorous framework to analyze the robustness, reliability, and predictability of fractional mathematical models, enabling deeper insights into their long-term behavior and practical applications. Applying the direct and inverse Sumudu transformation on both of the system (5), we obtain

$$\begin{cases} E_{RT}(t) = E_{RT}(0) + \mathbf{ST^{-1}}\Big\{\Psi.\mathbf{ST}\big[L^{\sigma-1}(-K_1 E_{RT}\mathcal{S}_{RNA} + (K_{-1}+K_2)C_1 - K_4 E_{RT}E_{IN} \\ \qquad +K_{-4}C_3)\big]\Big\}, \\ \mathcal{S}_{RNA}(t) = \mathcal{S}_{RNA}(0) + \mathbf{ST^{-1}}\Big\{\Psi.\mathbf{ST}\big[L^{\sigma-1}(-K_1 E_{RT}\mathcal{S}_{RNA} + K_{-1}C_1\big]\Big\}, \\ C_1(t) = C_1(0) + \mathbf{ST^{-1}}\Big\{\Psi.\mathbf{ST}\big[L^{\sigma-1}(K_1 E_{RT}\mathcal{S}_{RNA} - (K_{-1}+K_2)C_1)\big]\Big\}, \\ \mathcal{S}_{vDNA}(t) = \mathcal{S}_{vDNA}(0) + \mathbf{ST^{-1}}\Big\{\Psi.\mathbf{ST}\big[L^{\sigma-1}(K_2 C_1 - K_3\mathcal{S}_{vDNA}E_{IN} + K_{-3}C_2)\big]\Big\}, \\ E_{IN}(t) = E_{IN}(0) + \mathbf{ST^{-1}}\Big\{\Psi.\mathbf{ST}\big[L^{\sigma-1}(-K_3\mathcal{S}_{vDNA}E_{IN} + K_{-3}C_2 - K_4 E_{RT}E_{IN} \\ \qquad +K_{-4}C_3)\big]\Big\}, \\ C_2(t) = C_2(0) + \mathbf{ST^{-1}}\Big\{\Psi.\mathbf{ST}\big[L^{\sigma-1}(K_3\mathcal{S}_{vDNA}E_{IN} - K_{-3}C_2)\big]\Big\}, \\ C_3(t) = C_3(0) + \mathbf{ST^{-1}}\Big\{\Psi.\mathbf{ST}\big[L^{\sigma-1}(K_4 E_{RT}E_{IN} - K_{-4}C_3)\big]\Big\}, \end{cases} \tag{15}$$

where Ψ is the fractional Lagrange multiplier defined by,

$$\Psi = \frac{1-\sigma}{\mathbf{B}(\sigma)\left(\sigma\left(\Gamma(\sigma)+1\right)E_\sigma\left(-\frac{1}{1-\sigma}u^\sigma\right)\right)}.$$

Now we get the following iterative scheme,

$$\begin{cases}
E_{RT_{n+1}}(t) = E_{RT}(0) + \mathbf{ST^{-1}}\Big\{\Psi.\mathbf{ST}\big[L^{\sigma-1}(-K_1E_{RT_n}\mathcal{S}_{RNA_n} + (K_{-1}+K_2)C_{1_n} \\
\qquad -K_4E_{RT_n}E_{IN_n} + K_{-4}C_{3_n})\big]\Big\}, \\
\mathcal{S}_{RNA_{n+1}}(t) = \mathcal{S}_{RNA}(0) + \mathbf{ST^{-1}}\Big\{\Psi.\mathbf{ST}\big[L^{\sigma-1}(-K_1E_{RT_n}\mathcal{S}_{RNA_n} + K_{-1}C_{1_n})\big]\Big\}, \\
C_{1_{n+1}}(t) = C_1(0) + \mathbf{ST^{-1}}\Big\{\Psi.\mathbf{ST}\big[L^{\sigma-1}(K_1E_{RT_n}\mathcal{S}_{RNA_n} - (K_{-1}+K_2)C_{1_n})\big]\Big\}, \\
\mathcal{S}_{vDNA_{n+1}}(t) = \mathcal{S}_{vDNA}(0) + \mathbf{ST^{-1}}\Big\{\Psi.\mathbf{ST}\big[L^{\sigma-1}(K_2C_{1_n} - K_3\mathcal{S}_{vDNA_n}E_{IN_n} + K_{-3}C_{2_n})\big]\Big\}, \\
E_{IN_{n+1}}(t) = E_{IN}(0) + \mathbf{ST^{-1}}\Big\{\Psi.\mathbf{ST}\big[L^{\sigma-1}(-K_3\mathcal{S}_{vDNA_n}E_{IN_n} + K_{-3}C_{2_n} - K_4E_{RT_n}E_{IN_n} + \\
\qquad K_{-4}C_{3_n})\big]\Big\}, \\
C_{2_{n+1}}(t) = C_2(0) + \mathbf{ST^{-1}}\Big\{\Psi.\mathbf{ST}\big[L^{\sigma-1}(K_3\mathcal{S}_{vDNA_n}E_{IN_n} - K_{-3}C_{2_n})\big]\Big\}, \\
C_{3_{n+1}}(t) = C_3(0) + \mathbf{ST^{-1}}\Big\{\Psi.\mathbf{ST}\big[L^{\sigma-1}(K_4E_{RT_n}E_{IN_n} - K_{-4}C_{3_n})\big]\Big\}.
\end{cases}$$

Suppose $\mathbf{F}$ be a self-map on the Banach space $(\mathbb{H}, \|.\|)$ and consider the iteration $y_{n+1} = f(\mathbf{F}, y_n)$. Furthermore, let us assume $\mathcal{P}(\mathbf{F})$ be the fixed point set of $\mathbf{F}$ and $\{y_n\}$ converges to a some point $y \in \mathcal{P}(\mathbf{F})$. Suppose $Z_n = \{z_n\} \subseteq \mathbb{H}$ and defined by $\mathcal{N}_n = Z_{n+1} - f(\mathbf{F}, z_n)$. Suppose $\mathbf{F}$ be the self mapping defined as

$$\begin{cases}
\mathbf{F}\left(E_{RT_n}(t)\right) = E_{RT_{n+1}}(t) = E_{RT_n}(t) + \mathbf{ST^{-1}}\Big\{\Psi.\mathbf{ST}\big[L^{\sigma-1}(-K_1E_{RT_n}\mathcal{S}_{RNA_n} \\
\qquad +(K_{-1}+K_2)C_{1_n} - K_4E_{RT_n}E_{IN_n} + K_{-4}C_{3_n})\big]\Big\}, \\
\mathbf{F}\left(\mathcal{S}_{RNA_n}(t)\right) = \mathcal{S}_{RNA_{n+1}}(t) = \mathcal{S}_{RNA_n}(t) + \mathbf{ST^{-1}}\Big\{\Psi.\mathbf{ST}\big[L^{\sigma-1}(-K_1E_{RT_n}\mathcal{S}_{RNA_n} \\
\qquad +K_{-1}C_{1_n})\big]\Big\}, \\
\mathbf{F}\left(C_{1_n}(t)\right) = C_{1_{n+1}}(t) = C_{1_n}(t) + \mathbf{ST^{-1}}\Big\{\Psi.\mathbf{ST}\big[L^{\sigma-1}(K_1E_{RT_n}\mathcal{S}_{RNA_n} - (K_{-1}+K_2)C_{1_n})\big]\Big\}, \\
\mathbf{F}\left(\mathcal{S}_{vDNA_n}(t)\right) = \mathcal{S}_{vDNA_{n+1}}(t) = \mathcal{S}_{vDNA_n}(t) + \mathbf{ST^{-1}}\Big\{\Psi.\mathbf{ST}\big[L^{\sigma-1}(K_2C_{1_n} \\
\qquad -K_3\mathcal{S}_{vDNA_n}E_{IN_n} + K_{-3}C_{2_n})\big]\Big\}, \\
\mathbf{F}\left(E_{IN_n}(t)\right) = E_{IN_{n+1}}(t) = E_{IN_n}(t) + \mathbf{ST^{-1}}\Big\{\Psi.\mathbf{ST}\big[L^{\sigma-1}(-K_3\mathcal{S}_{vDNA_n}E_{IN_n} + K_{-3}C_{2_n} \\
\qquad -K_4E_{RT_n}E_{IN_n} + K_{-4}C_{3_n})\big]\Big\}, \\
\mathbf{F}\left(C_{2_n}(t)\right) = C_{2_{n+1}}(t) = C_{2_n}(t) + \mathbf{ST^{-1}}\Big\{\Psi.\mathbf{ST}\big[L^{\sigma-1}(K_3\mathcal{S}_{vDNA_n}E_{IN_n} - K_{-3}C_{2_n})\big]\Big\}, \\
\mathbf{F}\left(C_{3_n}(t)\right) = C_{3_{n+1}}(t) = C_{3_n}(t) + \mathbf{ST^{-1}}\Big\{\Psi.\mathbf{ST}\big[L^{\sigma-1}(K_4E_{RT_n}E_{IN_n} - K_{-4}C_{3_n})\big]\Big\}.
\end{cases} \tag{16}$$

Construct the following difference for the first population of our system in equation (16) as

$$\begin{aligned}
&\left\|\mathbf{F}\left(E_{RT_n}(t)\right) - \mathbf{F}\left(E_{RT_m}(t)\right)\right\| \\
=&\Big\|E_{RT_n}(t) - E_{RT_m}(t) + \mathbf{ST^{-1}}\Big\{\Psi.\mathbf{ST}\big[L^{\sigma-1} \\
&(-K_1E_{RT_n}\mathcal{S}_{RNA_n} + (K_{-1}+K_2)C_{1_n} - K_4E_{RT_n}E_{IN_n} + K_{-4}C_{3_n})\big]\Big\} - \mathbf{ST^{-1}}\Big\{\Psi.\mathbf{ST}
\end{aligned}$$

$$\begin{aligned}
&\big[L^{\sigma-1}(-K_1E_{RT_m}\mathcal{S}_{RNA_m}+(K_{-1}+K_2)C_{1_m}-K_4E_{RT_m}E_{IN_m}+K_{-4}C_{3_m})\big]\Big\}\Big\|\\
=&\Big\|E_{RT_n}(t)-E_{RT_m}(t)+\mathbf{ST^{-1}}\Big\{\Psi.\mathbf{ST}\Big[L^{\sigma-1}\big(-K_1\mathcal{S}_{RNA_n}\\
&(E_{RT_n}-E_{RT_m})-K_1E_{RT_m}(\mathcal{S}_{RNA_n}-\mathcal{S}_{RNA_m})+(K_{-1}+K_2)(C_{1_n}-C_{1_m})\\
&-K_4E_{IN_n}(E_{RT_n}-E_{RT_m})-K_4E_{RT_m}(E_{IN_n}-E_{IN_m})+K_{-4}(C_{3_n}-C_{3_m})\big)\Big]\Big\}\Big\|.
\end{aligned}$$

Using the triangle inequality, we obtain

$$\begin{aligned}
&\|\mathbf{F}(E_{RT_n}(t))-\mathbf{F}(E_{RT_m}(t))\|\\
\le&\|E_{RT_n}(t)-E_{RT_m}(t)\|+\mathbf{ST^{-1}}\Bigg\{\Psi.\mathbf{ST}\Big[L^{\sigma-1}\big(\|-K_1\mathcal{S}_{RNA_n}(E_{RT_n}-E_{RT_m})\|+\\
&\|-K_1E_{RT_m}(\mathcal{S}_{RNA_n}-\mathcal{S}_{RNA_m})\|+\|(K_{-1}+K_2)(C_{1_n}-C_{1_m})\|+\|-K_4E_{IN_n}\\
&(E_{RT_n}-E_{RT_m})\|+\|-K_4E_{RT_m}(E_{IN_n}-E_{IN_m})\|+\|K_{-4}(C_{3_n}-C_{3_m})\|\big)\Big]\Bigg\}.
\end{aligned}\tag{17}$$

As all the solutions E_{RT_n}, $\mathcal{S}_{RNA_n}$, C_{1_n}, $\mathcal{S}_{vDNA_n}$, E_{IN_n}, C_{2_n} and C_{3_n} are the Cauchy sequences in the Banach space $(\mathbb{H},\|.\|)$, and it is true that $\|E_{RT_n}(t)-E_{RT_m}(t)\|\to 0$, $\|\mathcal{S}_{RNA_n}(t)-\mathcal{S}_{RNA_m}(t)\|\to 0$, $\|C_{1_n}(t)-C_{1_m}(t)\|\to 0$, $\|\mathcal{S}_{vDNA_n}(t)-\mathcal{S}_{vDNA_m}(t)\|\to 0$, $\|E_{IN_n}(t)-E_{IN_m}(t)\|\to 0$, $\|C_{2_n}(t)-C_{2_m}(t)\|\to 0$ and $\|C_{3_n}(t)-C_{3_m}(t)\|\to 0$ as $n,m\to\infty$. Due to this similar behavior of the solutions, i.e., comparative influence of the solution in [30], we obtain

$$\begin{cases}
\|E_{RT_n}(t)-E_{RT_m}(t)\|\cong\|\mathcal{S}_{RNA_n}(t)-\mathcal{S}_{RNA_m}(t)\|,\\
\|E_{RT_n}(t)-E_{RT_m}(t)\|\cong\|C_{1_n}(t)-C_{1_m}(t)\|,\\
\|E_{RT_n}(t)-E_{RT_m}(t)\|\cong\|\mathcal{S}_{vDNA_n}(t)-\mathcal{S}_{vDNA_m}(t)\|,\\
\|E_{RT_n}(t)-E_{RT_m}(t)\|\cong\|E_{IN_n}(t)-E_{IN_m}(t)\|,\\
\|E_{RT_n}(t)-E_{RT_m}(t)\|\cong\|C_{2_n}(t)-C_{2_m}(t)\|,\\
\|E_{RT_n}(t)-E_{RT_m}(t)\|\cong\|C_{3_n}(t)-C_{3_m}(t)\|.
\end{cases}\tag{18}$$

Applying the congruence relation in the equation (18) on the inequality (17), we have

$$\begin{aligned}
&\|\mathbf{F}(E_{RT_n}(t))-\mathbf{F}(E_{RT_m}(t))\|\\
&\le\|E_{RT_n}(t)-E_{RT_m}(t)\|+\mathbf{ST^{-1}}\Bigg\{\Psi.\mathbf{ST}\Big[L^{\sigma-1}\big(\|-K_1\mathcal{S}_{RNA_n}(E_{RT_n}-E_{RT_m})\|+\\
&\|-K_1E_{RT_m}(E_{RT_n}-E_{RT_m})\|+\|(K_{-1}+K_2)(E_{RT_n}-E_{RT_m})\|+\|-K_4E_{IN_n}\\
&(E_{RT_n}-E_{RT_m})\|+\|-K_4E_{RT_m}(E_{RT_n}-E_{RT_m})\|+\|K_{-4}(E_{RT_n}-E_{RT_m})\|\big)\Big]\Bigg\}\\
&\le\|E_{RT_n}(t)-E_{RT_m}(t)\|\Big[1-K_1L^{\sigma-1}(\mathbb{M}_1+\mathbb{M}_2)\phi_1(\sigma)+(K_{-1}+K_2)L^{\sigma-1}\phi_2(\sigma)-\\
&K_4L^{\sigma-1}(\mathbb{M}_1+\mathbb{M}_5)\phi_3(\sigma)+K_{-4}L^{\sigma-1}\phi_4(\sigma)\Big],
\end{aligned}$$

where $\phi_1(\sigma)$, $\phi_2(\sigma)$, $\phi_3(\sigma)$, $\phi_4(\sigma)$ are the function of $\mathbf{ST}^{-1}\{\Psi.\mathbf{ST}\}$ and $\|E_{RT_n}\|\le\mathbb{M}_1$, $\|\mathcal{S}_{RNA_n}\|\le\mathbb{M}_2$, $\|C_{1_n}\|\le\mathbb{M}_3$, $\|\mathcal{S}_{vDNA_n}\|\le\mathbb{M}_4$, $\|E_{IN_n}\|\le\mathbb{M}_5$, $\|C_{2_n}\|\le\mathbb{M}_6$ and $\|C_{3_n}\|\le\mathbb{M}_7$. Proceeding

similar arguments for the other population of our system in the equation (16), we have

$$\begin{cases} \|\mathbf{F}\left(\mathcal{S}_{RNA_n}(t)\right) - \mathbf{F}\left(\mathcal{S}_{RNA_m}(t)\right)\| \leq \|\mathcal{S}_{RNA_n}(t) - \mathcal{S}_{RNA_m}(t)\|\Big[1 - K_1L^{\sigma-1}(\mathbb{M}_1+\mathbb{M}_2)\phi_1(\sigma) \\ \qquad +K_{-1}L^{\sigma-1}\phi_5(\sigma)\Big], \\ \|\mathbf{F}\left(C_{1_n}(t)\right) - \mathbf{F}\left(C_{1_m}(t)\right)\| \leq \|C_{1_n}(t) - C_{1_m}(t)\|\Big[1 + K_1L^{\sigma-1}(\mathbb{M}_1+\mathbb{M}_2)\phi_1(\sigma) \\ \qquad -(K_{-1}+K_2)L^{\sigma-1}\phi_2(\sigma)\Big], \\ \|\mathbf{F}\left(\mathcal{S}_{vDNA_n}(t)\right) - \mathbf{F}\left(\mathcal{S}_{vDNA_m}(t)\right)\| \leq \|\mathcal{S}_{vDNA_n}(t) - \mathcal{S}_{vDNA_m}(t)\|\Big[1 + K_2L^{\sigma-1}\phi_6(\sigma) \\ \qquad -K_3(\mathbb{M}_4+\mathbb{M}_5)L^{\sigma-1}\phi_7(\sigma)K_{-3}L^{\sigma-1}\phi_8(\sigma)\Big], \\ \|\mathbf{F}\left(E_{IN_n}(t)\right) - \mathbf{F}\left(E_{IN_m}(t)\right)\| \leq \|E_{IN_n}(t) - E_{IN_m}\|\Big[1 - K_3L^{\sigma-1}(\mathbb{M}_4+\mathbb{M}_5)\phi_7(\sigma) + K_{-3}L^{\sigma-1} \\ \qquad \phi_8(\sigma) - K_4L^{\sigma-1}(\mathbb{M}_1+\mathbb{M}_5)\phi_3(\sigma) + K_{-4}L^{\sigma-1}\phi_4(\sigma)\Big], \\ \|\mathbf{F}\left(C_{2_n}(t)\right) - \mathbf{F}\left(C_{2_m}(t)\right)\| \leq \|C_{2_n}(t) - C_{2_m}(t)\|\Big[1 + K_3L^{\sigma-1}(\mathbb{M}_4+\mathbb{M}_5)\phi_7(\sigma) \\ \qquad -K_{-3}L^{\sigma-1}\phi_8(\sigma)\Big], \\ \|\mathbf{F}\left(C_{3_n}(t)\right) - \mathbf{F}\left(C_{3_m}(t)\right)\| \leq \|C_{3_n}(t) - C_{3_m}(t)\|\Big[1 + K_4L^{\sigma-1}(\mathbb{M}_1+\mathbb{M}_5)\phi_3(\sigma) \\ \qquad -K_{-4}L^{\sigma-1}\phi_4(\sigma)\Big]. \end{cases}$$

Where $\phi_5(\sigma), \phi_6(\sigma), \phi_7(\sigma), \phi_8(\sigma)$ are same as the function $\mathbf{ST}^{-1}\{\Psi.\mathbf{ST}\}$. According to the Picard stability condition, we choose $G = (0,0,0,0,0,0,0)$ and Let us assume that the relation,

$$\mathcal{L} = \begin{cases} 1 - K_1L^{\sigma-1}(\mathbb{M}_1+\mathbb{M}_2)\phi_1(\sigma) + (K_{-1}+K_2)L^{\sigma-1}\phi_2(\sigma) - K_4L^{\sigma-1}(\mathbb{M}_1+\mathbb{M}_5)\phi_3(\sigma) \\ \qquad +K_{-4}L^{\sigma-1}\phi_4(\sigma) < 1, \\ 1 - K_1L^{\sigma-1}(\mathbb{M}_1+\mathbb{M}_2)\phi_1(\sigma) + K_{-1}L^{\sigma-1}\phi_5(\sigma) < 1, \\ 1 + K_1L^{\sigma-1}(\mathbb{M}_1+\mathbb{M}_2)\phi_1(\sigma) - (K_{-1}+K_2)L^{\sigma-1}\phi_2(\sigma) < 1, \\ 1 + K_2L^{\sigma-1}\phi_6(\sigma) - K_3L^{\sigma-1}(\mathbb{M}_4+\mathbb{M}_5)\phi_7(\sigma) + K_{-3}L^{\sigma-1}\phi_8(\sigma) < 1, \\ 1 - K_3L^{\sigma-1}(\mathbb{M}_4+\mathbb{M}_5)\phi_7(\sigma) + K_{-3}L^{\sigma-1}\phi_8(\sigma) - K_4L^{\sigma-1}(\mathbb{M}_1+\mathbb{M}_5)\phi_3(\sigma) \\ \qquad +K_{-4}L^{\sigma-1}\phi_4(\sigma) < 1, \\ 1 + K_3L^{\sigma-1}(\mathbb{M}_4+\mathbb{M}_5)\phi_7(\sigma) - K_{-3}L^{\sigma-1}\phi_8(\sigma) < 1, \\ 1 + K_4L^{\sigma-1}(\mathbb{M}_1+\mathbb{M}_5)\phi_3(\sigma) - K_{-4}L^{\sigma-1}\phi_4(\sigma) < 1. \end{cases} \tag{19}$$

Since the self-mapping $\mathbf{F}$ defined in the equation (16) has a fixed point and according to the Picard stability theorem if the conditions (19) are satisfied, the self-mapping $\mathbf{F}$ is Picard F-stable. Summarizing all the previous discussion, we now present the following theorem:

Theorem 5.1. *Considering the system with Atangana-Baleanu in the Caputo sense (7) along with the set of equation (15) and let* $\mathbf{F}$ *be the self-mapping defined by the equation in (16). If the conditions in (19) are all satisfied then the mapping* $\mathbf{F}$ *has a fixed point and hence* $\mathbf{F}$ *is Picard F-stable.*

Remark: The stability analysis of the fractional-order model confirms that small perturbations

in enzymatic reaction rates do not lead to unbounded changes in viral DNA or PIC levels over time. This reflects the biological resilience of HIV replication processes, where RT and IN interactions maintain functional balance even under molecular fluctuations. Specifically, the use of the ABC fractional operator demonstrates that memory effects contribute to this stability, reinforcing the models ability to capture persistent enzyme behavior critical to sustained viral integration.

§6 Computational analysis of our molecular system

This section presents the numerical interpretation of our mathematical model (both integer-order as well as fractional-order) using Matlab 2021a. We begin this section by simulating the sensitivity index of the integer-order model using Latin Hypercube Sampling (LHS), which illustrates the impact of model parameters on the system's dynamics. Subsequently, we incorporate fractional-order dynamics to analyze the memory effects on the biochemical and physical interactions between RT and IN enzymes. Here, we explore the dynamics of the three fractional-order systems with respect to three different kernels: Caputo, Caputo-Fabrizio and Atangana-Baleanu in the Caputo sense. We consider biologically plausible parameter values and estimate additional parameters from available clinical and experimental literature. The parameter values are summarized in Table 1.

6.1 Sensitivity analysis of reaction parameter

Sensitivity analysis (SA) plays a vital role in quantifying the uncertainty of model parameters and evaluating how variations in these parameters influence the model's outcomes. Local sensitivity analysis examines the effect of varying one parameter at a time, while keeping all other parameters fixed at their estimated values. However, this type of sensitivity analysis cannot provide comprehensive information about the model¡¯s outcomes or the sensitivity of its parameters. To address this limitation, we perform global sensitivity analysis using an efficient technique called LHS, as described by Marino et al. [31].

The LHS method is a type of Monte Carlo simulation first introduced by McKay et al. [32] in 1979. It ensures independent sampling for each parameter without replacement, following the probability density function (PDF). In this method, each parameter's range is divided into N intervals of equal probability, and one sample is randomly selected from each interval. This process generates a matrix of dimensions $N \times k$, where N is the sample size and k is the number of parameters. In this study, the number of parameters (p) is 7, with the sample size set to $N = 1000$.

Partial Rank Correlation Coefficient (PRCC) is an effective sampling-based statistical tool used for sensitivity analysis in complex models, especially in the context of LHS. It measures the correlation coefficient (CC) between input parameters and the model output while controlling for the effects of other parameters. The value of the correlation coefficient (CC), $r \in [-1, 1]$,

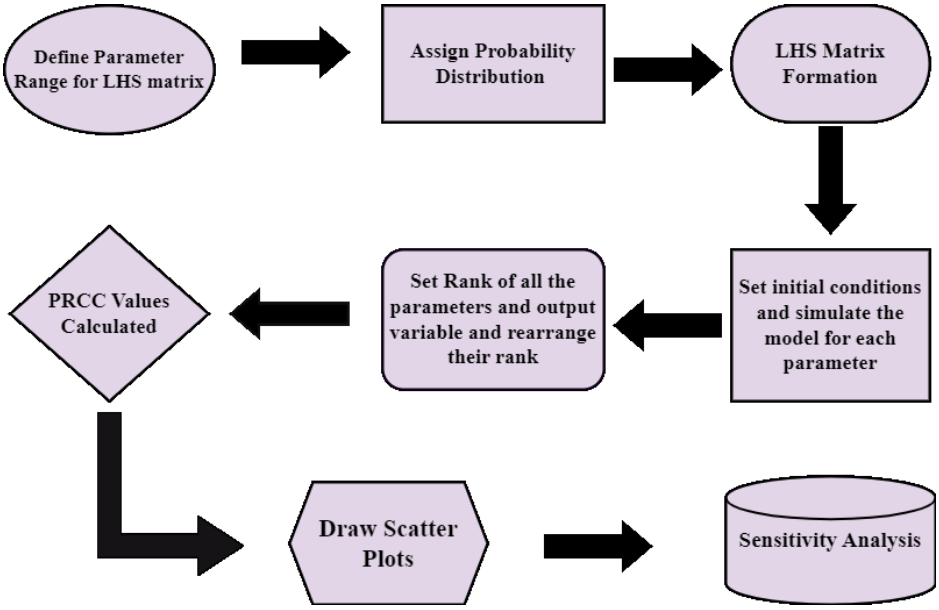

Figure 2. Step-by-step illustration of the LHS-PRCC method, presenting the detailed working procedure for performing a comprehensive global sensitivity analysis, including parameter sampling, correlation computation, and interpretation of results to identify influential parameters.

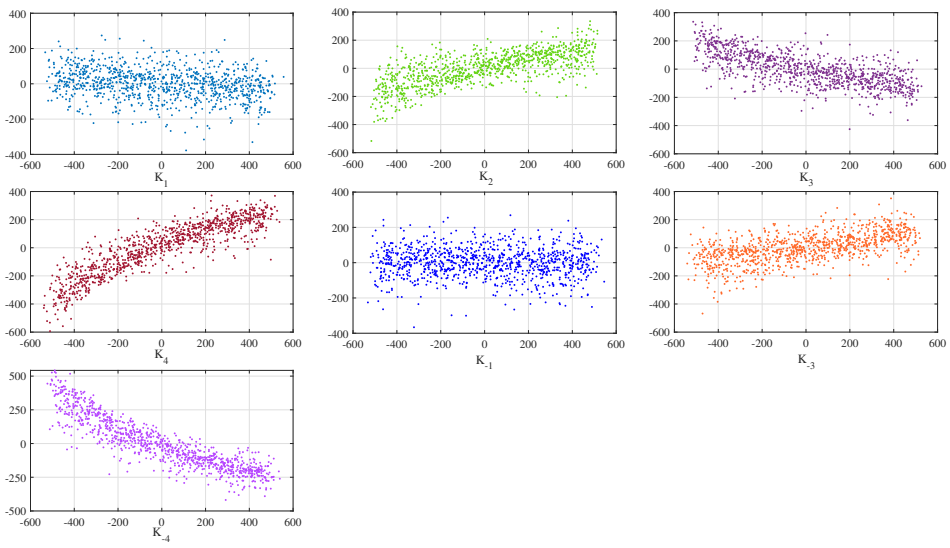

Figure 3. Scatter plot for the output variable viral DNA ($\mathcal{S}_{vDNA}$) with respect to all reaction rates. The range of input variables (all reaction rates) are taken as in the Table 1. The x-axis shows the residuals obtained from regressing the rank-transformed values of the parameter of interest on the rank-transformed values of all other parameters. The y-axis displays the residuals from regressing the rank-transformed values of viral DNA on the rank-transformed values of all other parameters, excluding the one being analyzed.

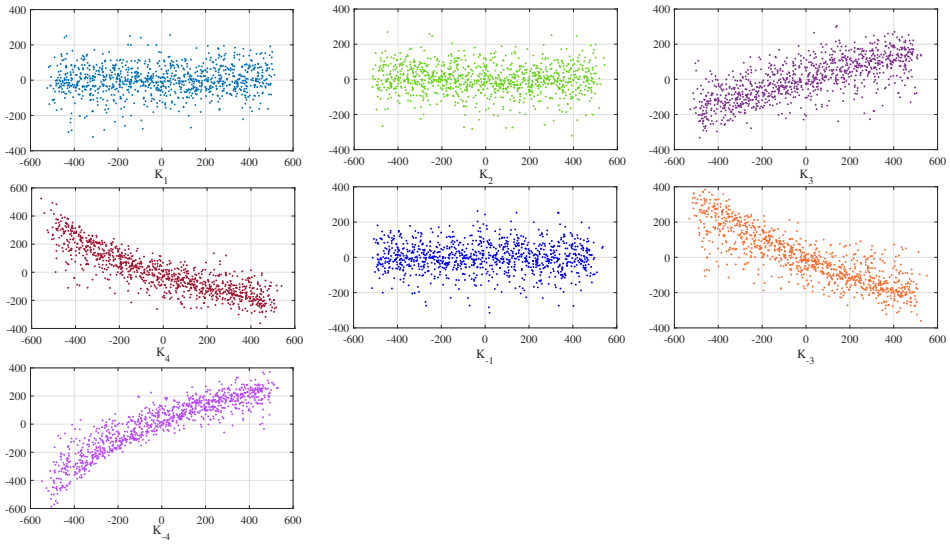

Figure 4. Scatter plot for the output variable Pre-Integration complex (C_2) with respect to all reaction rates. The range of input variables (all reaction rates) are taken as in the Table 1. The x-axis shows the residuals obtained from regressing the rank-transformed values of the parameter of interest on the rank-transformed values of all other parameters. The y-axis displays the residuals from regressing the rank-transformed values of PIC on the rank-transformed values of all other parameters, excluding the one being analyzed.

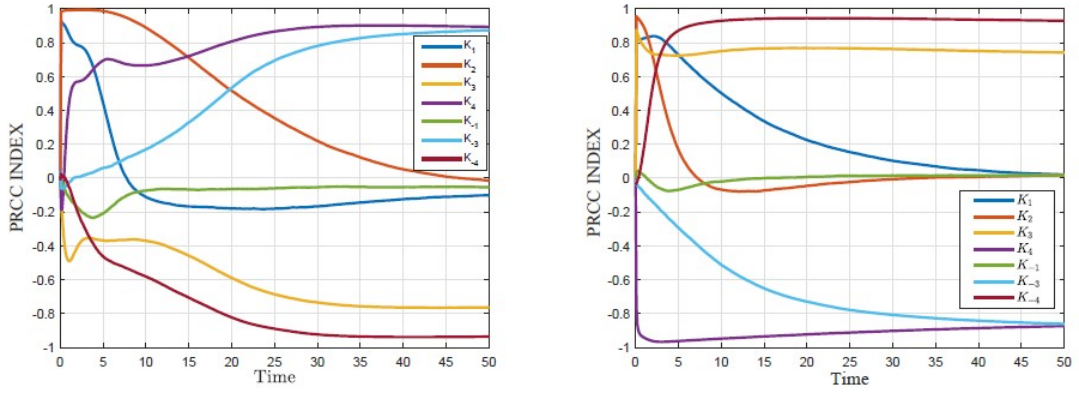

Figure 5. Changes of PRCC value of all reaction rates with respect to time. (a) Changes of PRCC with respect to the output variable viral DNA and (b) Changes of PRCC with respect to the output variable Pre-integration complex. The ranges of all reaction rates are consider as in the table 1.

for an input variable (X) and output variable (Y) is calculated as follows:

$$r = \frac{Cov(X,Y)}{\sqrt{Var(X)Var(Y)}} = \frac{\sum(X-\bar{X})(Y-\bar{Y})}{\sqrt{\sum(X-\bar{X})^2\sum(Y-\bar{Y})^2}},$$

where $\bar{X}$ and $\bar{Y}$ represent the corresponding sample means of X and Y, respectively. All reaction rates are taken as input variables, and viral double-stranded DNA and the PIC are considered only as output variables for simulating correlation coefficients.

Our aim in this study is to understand how the reactions of RT and IN enzymes regulate the production of viral DNA and the formation of the PIC. We perform global sensitivity analysis using the LHS-PRCC method and the algorithm, the details of which are given in the schematic Fig. 2. The sensitivity analysis is visualized through the scatter plots 3 and 4. We calculate the PRCC value and p-value for each parameter, which are given in Table 2. The PRCC value denotes the direct correlation between the output variables (here, viral DNA and PIC) and all the model parameters. The p-value represents the level of uncertainty related to each PRCC value and is calculated. PRCC value with a p-value < 0.05 signifies significance in the statistical testing. Here, we consider the p-value for all reaction rates accurate up to four decimal places.

In Fig. 3, we represent the sensitivity between the production of viral DNA and all reaction parameters. The figure shows that the reaction rates K_2, K_4, K_{-3} are positively influential parameters, while other reaction rates K_1, K_3, K_{-1}, K_{-4} are negatively influential parameters for the production of viral DNA. Similarly, the sensitivity between the formation of the PIC and all the reaction rates is showcased in Fig. 4, where the reaction rates K_1, K_3, and K_{-4} are positively influential and K_2, K_4, K_{-1}, and K_{-3} are negatively influential parameters for the formation of the PIC.

Table 2. PRCC and p-values of all reaction parameters with respect to Viral DNA and the pre-integration complex as output variables using the Spearman method. Here we calculate all PRCC values upto four decimal significant figures.

Reaction Parameters	Viral DNA as output		Pre integration complex as output	
	PRCC value	P-Value	PRCC value	P-Value
K_1	-0.2566	9.342812e-14	0.0689	6.498099e-03
K_2	0.7012	0.000000e+00	-0.0544	5.550342e-02
K_3	-0.7010	0.000000e+00	0.7385	0.000000e+00
K_4	0.8990	0.000000e+00	-0.8624	0.000000e+00
K_{-1}	-0.0359	2.760711e-02	-0.0211	7.622725e-02
K_{-3}	0.5981	0.000000e+00	-0.8496	0.000000e+00
K_{-4}	-0.9112	0.000000e+00	0.9184	0.000000e+00

In Figs. 3 and 4, we only study the global sensitivity analysis (GSA) at t = 50 hours. However in order to focus on sensitivity, performing GSA at a single time does not provide a comprehensive view of how all reaction rates affect the outcomes. In order to gain a more profound understanding of the behavior of the reaction rates, we perform the GSA in the whole time span in Fig. 5. Fig. 5 illustrates that the PRCC value of all reaction rates changes across the two important compartment of our system as viral DNA and PIC changes over time.

This changing tendency of the specific parameters across different compartments reveals the significant variation in the system results.

In the Fig. 5a, we perform the sensitivity of each parameter with respect to viral DNA over time. Initially the fluctuation of the PRCC value of reaction rate indicates that the varying sensitivity of each reaction rates for the production of viral DNA. At the initial stage of reaction, K_1 and K_2 show positive in the production of viral DNA but their positive influence diminishes over time. Most interestingly, K_2 becomes negative influential over time. Meanwhile, K_4 and K_{-3} represent the reciprocal result, i.e., they are change from negative influence to positive influence with respect to viral DNA.

Fig. 5b illustrates about the sensitivity of reaction rates for the formation of PIC. The reaction rates K_1, K_2, K_4 and K_{-3} are shown similar behavior as the Fig. 5a for the formation of PIC over time. However, in this Fig. 5b, two other phenomena are noticeable: K_3 always maintains highly positive influential in the formation PIC, whereas K_{-4} becomes positively influential after some time following the initiation of the reaction.

6.2 Numerical representation for three different fractional model

In this section, we numerically interpret the results from our three fractional models. We represent the numerical scheme to solve the fractional model. We present a numerical scheme to solve the fractional model based on the Atangana-Baleanu operator, Caputo and Caputo-Fabrizio. To explain this numerical solution, we consider the fractional system (5) in the following form

$$L^{(1-\sigma)\ {}^{ABC}}D_t^{\sigma}(f(t)) = \phi(f(t),t), \tag{20}$$

where $f(t) = [E_{RT}, \mathcal{S}_{RNA}, C_1, \mathcal{S}_{vDNA}, E_{IN}, C_2, C_3]^T$ and $\phi(f(t),t)$ denotes the right side of the system (5). Utilizing the fundamental theorem of fractional calculus in (20), we obtain

$$f(t) - f(0) = \frac{L^{(\sigma-1)}(1-\sigma)}{\mathbf{B}(\sigma)}\phi(f(t),t) + \frac{L^{(\sigma-1)}\sigma}{\mathbf{B}(\sigma)\Gamma(\sigma)}\int_0^t (t-\xi)^{(\sigma-1)}\phi(f(\xi),\xi)d\xi. \tag{21}$$

where $\mathbf{B}(\sigma) = 1-\sigma+\frac{\sigma}{\Gamma(\sigma)}$ is a normalization function. Putting $t = t_{n+1} = (n+1)h$ in equation (21), where h is the time step size

$$\begin{aligned} f(t_{n+1}) - f(0) &= \frac{L^{(\sigma-1)}(1-\sigma)}{\mathbf{B}(\sigma)}\phi(f(t_n),t_n) + \frac{L^{(\sigma-1)}\sigma}{\mathbf{B}(\sigma)\Gamma(\sigma)}\int_0^{t_{n+1}} (t_{n+1}-\xi)^{(\sigma-1)}\phi(f(\xi),\xi)d\xi \\ &= \frac{L^{(\sigma-1)}(1-\sigma)}{\mathbf{B}(\sigma)}\phi(f(t_n),t_n) \\ &\quad + \frac{L^{(\sigma-1)}\sigma}{\mathbf{B}(\sigma)\Gamma(\sigma)}\sum_{m=0}^{n}\int_{t_m}^{t_{m+1}} (t_{n+1}-\xi)^{(\sigma-1)}\phi(f(\xi),\xi)d\xi. \end{aligned} \tag{22}$$

Using the second step Lagrange interpolation polynomial, the function ϕ approximates to

$$\phi(f(\xi),\xi) \approx \frac{\phi(f(t_m),t_m)}{h}(\xi - t_{m-1}) - \frac{\phi(f(t_{m-1}),t_{m-1})}{h}(\xi - t_m). \tag{23}$$

Using this result in (23) on the equation (22), we have

$$\begin{aligned}
f(t_{n+1}) =& f(0) + \frac{L^{(\sigma-1)}(1-\sigma)}{\mathbf{B}(\sigma)}\phi(f(t_n),t_n) \\
&+ \frac{L^{(\sigma-1)}\sigma}{\mathbf{B}(\sigma)\Gamma(\sigma)}\sum_{m=0}^{n}\left[\frac{\phi(f(t_m),t_m)}{h}\int_{t_m}^{t_{m+1}}(t_{n+1}-\xi)^{(\sigma-1)}(\xi-t_{m-1}))d\xi\right. \\
&\left.- \frac{\phi(f(t_{m-1}),t_{m-1})}{h}\int_{t_m}^{t_{m+1}}(t_{n+1}-\xi)^{(\sigma-1)}(\xi-t_m))d\xi\right] \\
=& f(0) + \frac{L^{(\sigma-1)}(1-\sigma)}{\mathbf{B}(\sigma)}\phi(f(t_n),t_n) + \frac{L^{(\sigma-1)}\sigma}{\mathbf{B}(\sigma)\Gamma(\sigma)}\sum_{m=0}^{n}\left[\frac{\phi(f(t_m),t_m)}{h}\times\frac{h^{\sigma+1}}{\sigma(\sigma+1)}\right. \\
&\times\left((n-m+1)^{\sigma}(n-m+\sigma+2)-(n-m)^{\sigma}(n-m+2\sigma+2)\right) \\
&\left.- \frac{\phi(f(t_{m-1}),t_{m-1})}{h}\times\frac{h^{\sigma+1}}{\sigma(\sigma+1)}\left((n-m+1)^{\sigma+1}-(n-m)^{\sigma}(n-m+\sigma+1)\right)\right] \\
=& f(0) + \frac{L^{(\sigma-1)}(1-\sigma)}{\mathbf{B}(\sigma)}\phi(f(t_n),t_n) + \frac{L^{(\sigma-1)}h^{\sigma}}{\mathbf{B}(\sigma)\Gamma(\sigma)(\sigma+1)}\sum_{m=0}^{n}\left[\left((n-m+1)^{\sigma}(n-m\right.\right. \\
&\left.+\sigma+2)-(n-m)^{\sigma}(n-m+2\sigma+2)\right)\phi(f(t_m),t_m) - \left((n-m+1)^{\sigma+1}\right. \\
&\left.\left.-(n-m)^{\sigma}(n-m+\sigma+1)\right)\phi(f(t_{m-1}),t_{m-1})\right].
\end{aligned}$$

Apply this numerical scheme in the system (5) for every model population, which we use in this numerical section part. Similarly, we find the numerical scheme for the Caputo fractional model (3). So we can not be shown detailed calculations for the Caputo scheme. The fractional model corresponding to Caputo derivative can be written as similar to equation (20)

$$L^{(1-\zeta)}\ {}^{C}D_t^{\zeta}(f(t)) = \phi(f(t),t). \tag{24}$$

Applying the same procedure as the previous numerical solution of the fractional model corresponding to Atangana-Baleanu in the Caputo sense, we have the solution of equation (24) in the form

$$\begin{aligned}
f(t_{n+1}) =& f(0) + \frac{L^{(\zeta-1)}h^{\zeta}}{\Gamma(\zeta+1)}\sum_{m=0}^{n}\left[\left((n-m+1)^{\zeta}(n-m+\zeta+2)-(n-m)^{\zeta}(n-m+2\zeta+2)\right)\right. \\
&\left.\times\phi(f(t_m),t_m) - \left((n-m+1)^{\zeta+1}-(n-m)^{\zeta}(n-m+\zeta+1)\right)\phi(f(t_{m-1}),t_{m-1})\right].
\end{aligned} \tag{25}$$

Now we present the numerical solution of the fractional model corresponding to the Caputo-Fabrizio derivative scheme. The fractional model (4) can be written in the following form

$$L^{(1-\alpha)}\ {}^{CF}D_t^{\alpha}(f(t)) = \phi(f(t),t), \tag{26}$$

where $f(t)$ and $\phi(f(t),t)$ denote same as in equation (20). Applying the fundamental theorem of fractional calculus in equations (26), we have

$$f(t)-f(0)=\frac{L^{\alpha-1}(1-\alpha)}{M(\alpha)}\phi(f(t),t)+\frac{L^{\alpha-1}\alpha}{M(\alpha)}\int_0^t\phi(f(\xi),\xi)d\xi. \tag{27}$$

Taking $t=t_{n+1}$ and $t=t_n$ in equation (27), we obtain

$$f(t_{n+1})-f(0)=\frac{L^{\alpha-1}(1-\alpha)}{M(\alpha)}\phi(f(t_n),t_n)+\frac{L^{\alpha-1}\alpha}{M(\alpha)}\int_0^{t_{n+1}}\phi(f(\xi),\xi)d\xi,\quad \text{and} \tag{28}$$

$$f(t_n)-f(0)=\frac{L^{\alpha-1}(1-\alpha)}{M(\alpha)}\phi(f(t_{n-1}),t_{n-1})+\frac{L^{\alpha-1}\alpha}{M(\alpha)}\int_0^{t_n}\phi(f(\xi),\xi)d\xi. \tag{29}$$

From equations (28) and (29), we have

$$f(t_{n+1})=f(t_n)+\frac{L^{\alpha-1}(1-\alpha)}{M(\alpha)}\Big(\phi(f(t_n),t_n)-\phi(f(t_{n-1}),t_{n-1})\Big)+\frac{L^{\alpha-1}\alpha}{M(\alpha)}\int_{t_n}^{t_{n+1}}\phi(f(\xi),\xi)d\xi. \tag{30}$$

Applying the approximated solution of $\phi(f(\xi),\xi)$ in equation (23), we have

$$\begin{aligned}\int_{t_n}^{t_{n+1}}\phi(f(\xi),\xi)d\xi&=\int_{t_n}^{t_{n+1}}\left[\frac{\phi(f(t_n),t_n)}{h}(\xi-t_{n-1})-\frac{\phi(f(t_{n-1}),t_{n-1})}{h}(\xi-t_n)\right]d\xi\\&=\frac{3h}{2}\phi(f(t_n),t_n)-\frac{h}{2}\phi(f(t_{n-1}),t_{n-1}).\end{aligned} \tag{31}$$

Utilizing this result in equation (31) to the equation (30), we get

$$f(t_{n+1})=f(t_n)+\frac{L^{\alpha-1}}{M(\alpha)}\left[\big((1-\alpha)+\frac{3h\alpha}{2}\big)\phi(f(t_n),t_n)-\big((1-\alpha)+\frac{h\alpha}{2}\big)\phi(f(t_{n-1}),t_{n-1})\right]. \tag{32}$$

We utilize this numerical scheme to solve the fractional model (4) corresponding to the Caputo-Fabrizio fractional operator. The simulations shown in Figs. 7 and 10 are generated using this numerical method.

In Figs. 6-8, we demonstrate the influence of fractional order on the competitive molecular interactions between RT and IN enzymes. Fig. 6 illustrates how variations in the fractional order ζ affect the behavior of all molecular concentrations in our fractional model (3), while the memory rate parameter L is fixed at 0.7. Specifically, it highlights that the Caputo fractional differential operator produces only minor variations in molecular dynamics, indicative of its short-term memory effect.

In Fig. 7, we present the dynamic changes in the concentrations of all molecules in the Caputo-Fabrizio fractional model (4) corresponding to different values of the fractional order α, with the fixed value of the memory rate parameter $L=0.7$. The figure reveals a noticeable variation in the behavior of molecular concentrations, demonstrating the non-singular kernel's ability to capture moderate memory effects effectively.

For the fractional model (5) based on the Atangana-Baleanu operator in the Caputo sense, the variation of fractional order σ exhibits a significant impact on the dynamical behavior of all molecule concentrations, as shown in Fig. 8, while we fixed the value of the memory rate parameter $L=0.7$. This variation highlights the influence of the non-local and non-singular kernel, demonstrating its ability to capture complex molecular interactions and reflect long-term memory effects inherent in biological systems.

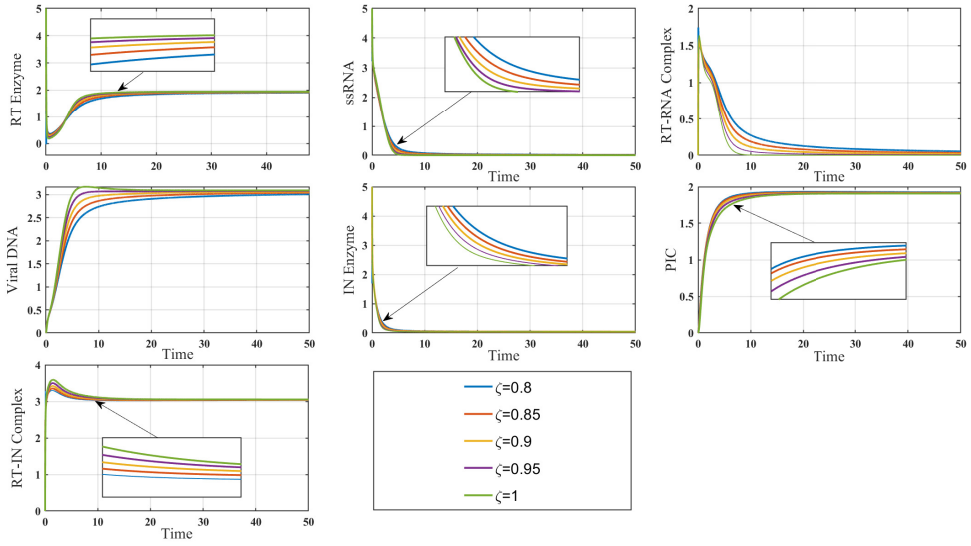

Figure 6. Dynamical behavior of all system populations corresponding to the Caputo fractional model. Here we take five values of fractional order ζ as 0.8, 0.85, 0.9, 0.95 and 1. The value of all reaction rates is taken as $K_1 = 1$, $K_{-1} = 0.06$, $K_2 = 0.5$, $K_3 = 1.1$, $K_{-3} = 0.07$, $K_4 = 1$, $K_{-4} = 0.05$. Initial conditions are taken as $E_{RT}(0) = 5$, $\mathcal{S}_{RNA}(0) = 5$, $C_1(0) = 0$, $\mathcal{S}_{vDNA}(0) = 0$, $E_{IN}(0) = 5$, $C_2(0) = 0$ and $C_3(0) = 0$

.

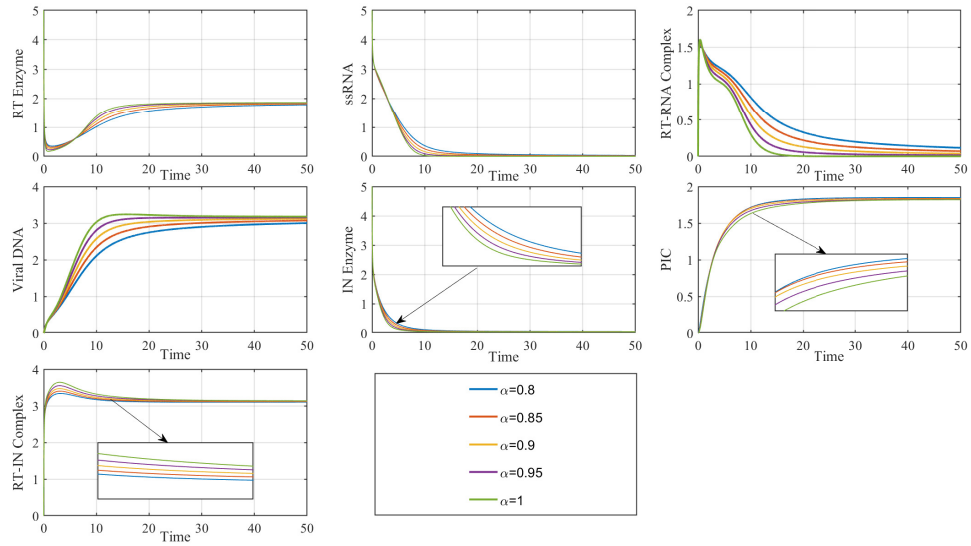

Figure 7. Dynamical changes of all system populations corresponding to the Caputo-Fabrizio fractional model. Here we take five values of fractional order α as 0.8, 0.85, 0.9, 0.95 and 1. All the values of reaction rates and initial conditions of all model populations are taken the same as Fig. 6.

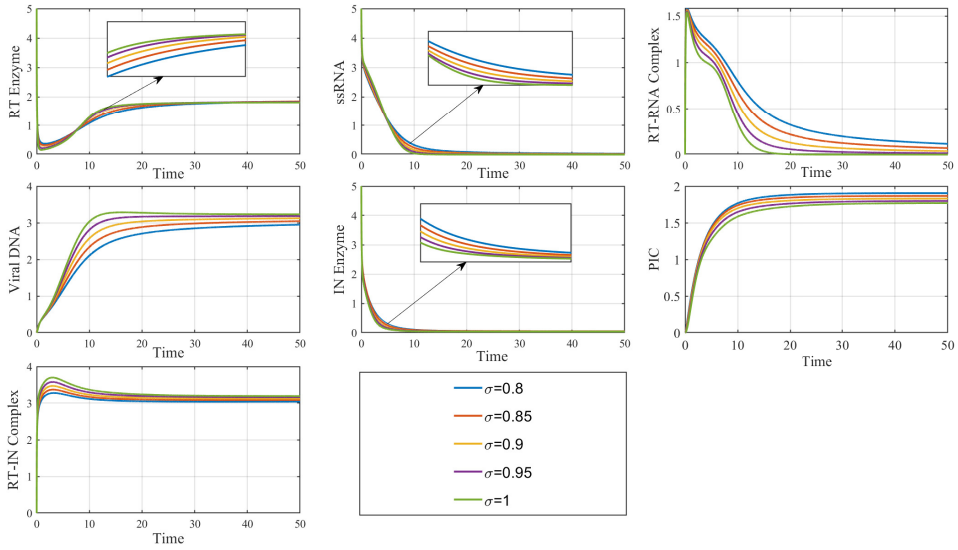

Figure 8. Dynamical changes of all system populations corresponding to the Atangana-Baleanu in the Caputo sense fractional model. Here we take five values of fractional order σ as 0.8, 0.85, 0.9, 0.95 and 1. All the values of reaction rates and initial conditions of all system populations are taken the same as Fig. 6.

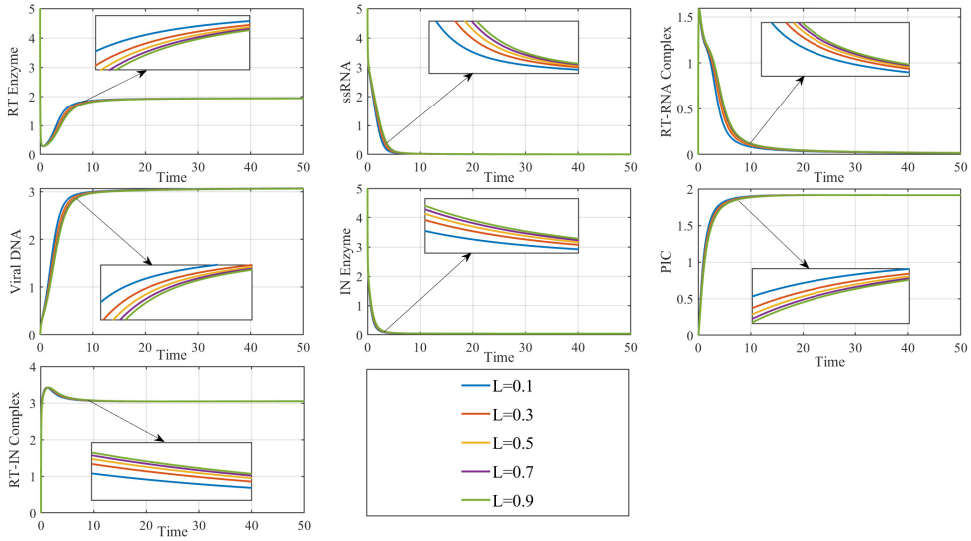

Figure 9. Dynamical behavior of all system populations in the Caputo fractional model, shown with variations in the memory rate parameter L, while keeping the fractional order fixed at $\zeta = 0.9$. Reaction parameter values are consistent with those in Fig. 6.

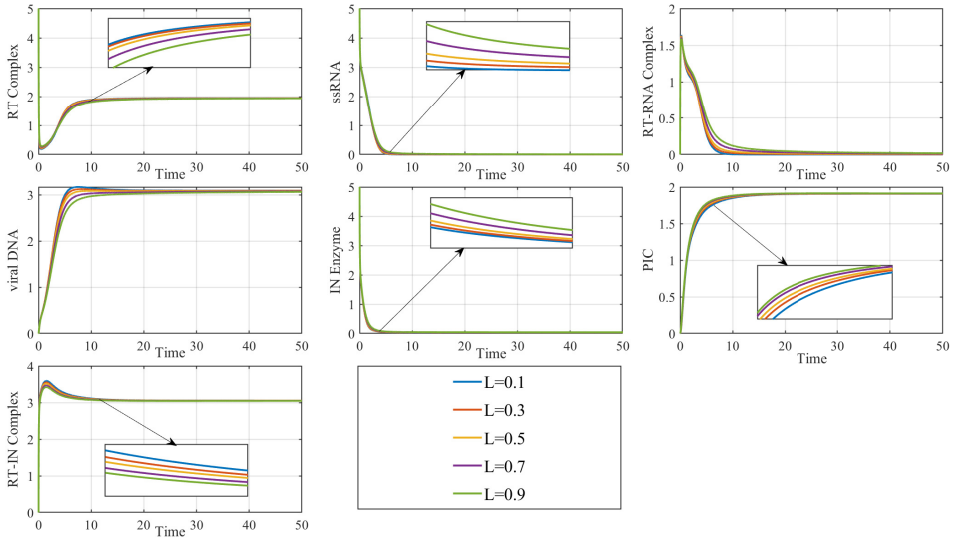

Figure 10. Effect of varying the memory rate parameter L on the dynamical behavior of all system populations in the Caputo fractional model, with the fractional order fixed at $\alpha = 0.9$. The values of all reaction parameters are taken from the Table 1.

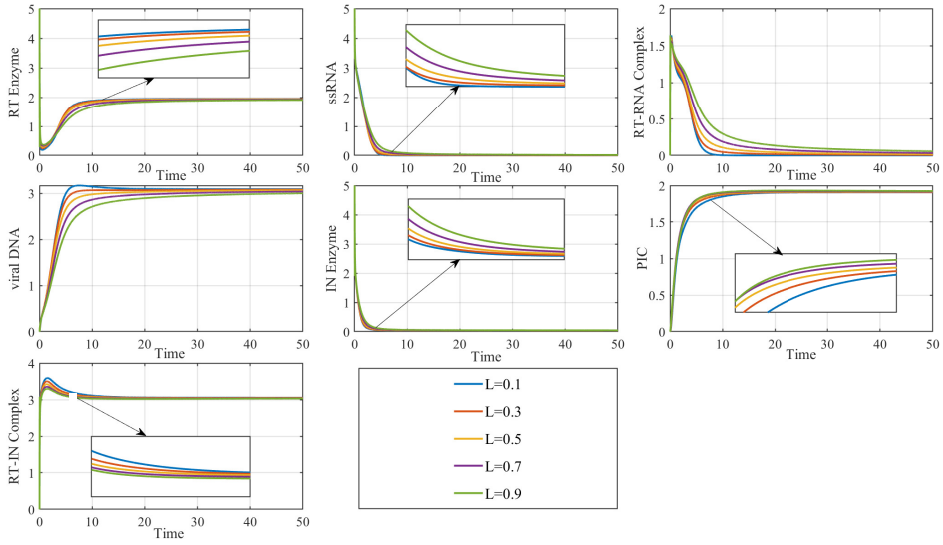

Figure 11. Changes in the concentration of all molecules in the fractional system corresponding to the Atangana Baleanu in the Caputo sense operator with respect to variations in the memory rate parameter L at values of 0.1, 0.3, 0.5, 0.7, and 0.9, while the fractional order is fixed at $\sigma = 0.9$. Values of all reaction rate parameters are the same as those in the previous figures.

In Figs. 9-11, we illustrate the effect of the variation in the memory rate parameter L on the dynamics of the biological system within our time-fractional mathematical model for three distinct fractional operators. Fig. 9 highlights the system's behavior as the memory rate parameter L varies, while the fractional order remains fixed at $\zeta = 0.9$. The results emphasize how changes in the memory rate influence molecular dynamics, demonstrating shorter memory effects characteristic of the singular kernel associated with the Caputo fractional operator.

Fig. 10 illustrates the dynamic changes in all system populations within the Caputo-Fabrizio fractional model (4) for varying values of the memory rate parameter L, while the fractional order is fixed at $\alpha = 0.9$. Similarly, Fig. 11 demonstrates the system behaviors for the fractional model corresponding to the ABC method with L variations, revealing significant shifts in molecular interactions. This figure highlights the non-local and non-singular kernel properties of the Atangana-Baleanu operator, effectively capturing long-term memory effects and showcasing its suitability for modeling the complexity inherent in biological systems.

§7 Discussion and Conclusion

Molecular interactions in HIV replication play a key role in infecting host cells and producing new virus particles. These interactions are essential for developing effective and targeted antiretroviral therapies. In this study, we highlight two parallel molecular interactions between RT and IN enzymes, known as biochemical interaction and physical interaction, which inhibit each other. To investigate the interplay between these two interactions more precisely, we consider a seven-dimensional kinetic mathematical model under three different fractional-order differential operators: Caputo, Caputo-Fabrizio, and Atangana-Baleanu in the Caputo sense.

This study has some limitations. We focused only on how the RT and IN enzymes interact to form viral DNA and the pre-integration complex, without including other important proteins or host cell factors. Additionally, while most reaction parameters were based on experimental studies, a few were estimated in the absence of direct data. Although our sensitivity analysis identifies potential therapeutic targets such as the RT-IN complex, the model has not been fully validated using empirical or clinical time-series data. These limitations are acknowledged in the manuscript and guide future directions for enhancing the model's translational value.

We established the existence and uniqueness of all system solutions for the ABC-induced mathematical model using fixed-point theory in Section 4. Additionally, we analyzed the stability of the fractional model using Picard stability theory in Section 5. In Subsection 6.1, we performed a global sensitivity analysis of all reaction parameters and calculated the PRCC values, as shown in Figs. 3-5. The analysis identifies the reaction parameters K_3 and K_4, which are highlighted as critical factors in the dynamics of viral DNA and the pre-integration complex. These findings demonstrate that the reaction rate K_3 and K_4 significantly influence viral DNA synthesis and PIC formation, indicating that targeting these reactions may improve the effectiveness of HIV therapies by inhibiting key stages of viral integration.

We numerically analyzed the behavior of the system across all population variables in Figs.

6-8 by varying the fractional-order values and employing three distinct kernels: Caputo, Caputo-Fabrizio, and ABC in Subsection 6.2. These simulations provided a detailed exploration of how fractional dynamics influence the system, revealing the unique impact of each kernel on system dynamics. The results reveal that the ABC kernel, due to its non-local and non-singular properties, captures long-term memory effects more effectively than the Caputo and Caputo-Fabrizio models, leading to stronger suppression of viral DNA and PIC levels at lower fractional orders.

Additionally, we illustrated the local and non-local system dynamics in Figs. 9-11 by varying the memory rate parameter. These figures provide a complex representation of biological processes influenced by historical states, enabling a realistic depiction of complex, non-Markovian behaviors inherent in such systems. The memory-driven dynamics of molecular interactions, particularly the physical interactions inhibiting biochemical processes, are explored through fractional calculus, providing deeper insights into the time-dependent processes in HIV replication. This study bridges molecular study and fractional calculus, revealing critical factors that influence enzyme activity and identifying potential intervention points for HIV treatment.

Our model identifies the physical interaction between RT and IN as a critical regulatory mechanism in HIV replication, a result supported by experimental evidence from Masuda et al. (2022), who demonstrated that integrase modulates RT activity through cis-allosteric interactions affecting its conformation and function [16]. Additionally, our sensitivity analysis highlights parameters related to strand transfer and RT-IN complex formation as key influencers of viral DNA and PIC dynamics. This finding aligns with clinical findings that strand transfer inhibitors like Raltegravir effectively suppress HIV replication by blocking integration into the host genome [33, 34]. The fractional-order modeling further reveals memory-driven effects in these enzymatic processes, reflecting observed delayed responses in antiretroviral therapies such as Cabenuva, a long-acting regimen shown to maintain suppression over extended periods [35]. These connections between our numerical results and biological data reinforce the validity of the model and underscore its translational potential in guiding targeted, time-sensitive HIV treatments.

Beyond its theoretical and computational contributions, the proposed fractional-order modeling framework carries meaningful translational potential. By elucidating the interplay between RT and IN through both biochemical and physical pathways and quantifying their roles via memory-sensitive parameters, our model offers insights into how fractional dynamics influence HIV replication. These insights can be instrumental in the rational design of next-generation antiretroviral therapies. Specifically, our findings advocate for a shift toward targeting the RT-IN complex rather than solely focusing on integrase-DNA interactions. This approach could inform drug discovery pipelines and support the development of inhibitors that modulate enzymatic interactions with inherent memory effects. Furthermore, integrating this modeling framework into preclinical evaluation may enhance therapeutic efficacy by guiding dose optimization and improving the clinical utility of memory-aware antiviral strategies.

Building on our current findings, future research will incorporate the effects of antiretroviral

drugs on both biochemical and physical RT-IN interactions within the fractional-order modeling framework. This will allow a more precise investigation of how drug-induced perturbations influence system memory, enzyme activity, and viral suppression. Additionally, integrating clinical data and employing parameter estimation techniques will enable empirical validation of the model, enhancing its translational potential for optimizing HIV treatment strategies and informing the development of next-generation therapies targeting memory-dependent molecular mechanisms.

Declarations

Conflict of interest The authors declare no conflict of interest.

References

[1] World Health Organization. *Global status report on HIV epidemic*, 2023, https://www.who.int-/ data/gho/data/themes/hiv-aids#: :text=Globally%2C%2039.9%20million%20%5B36.1%E2%-80%93,considerably%20between%20countries%20and%20regions.

[2] UNAIDS. *South Africa statistical report on HIV epidemic*, 2023, https://www.unaids.org/en/regionscountries/countries/southafrica.

[3] T Ghosh, P K Roy. *Critical analysis of FDA-approved dual inhibitor cabenuva to HIV replication kinetics: a mathematical study*, Mathematical Biology and Bioinformatics, 2025, 20(2): 236-268.

[4] P Zhan, X Liu, E D Clercq. *Blocking nuclear import of pre-integration complex: an emerging anti-HIV-1 drug discovery paradigm*, Current Medicinal Chemistry, 2010, 17(6): 495-503.

[5] T Tasara, G Maga, M O Hottiger, et al. *HIV-1 reverse transcriptase and integrase enzymes physically interact and inhibit each other*, FEBS Letters, 2001, 507(1): 39-44.

[6] T A Wilkinson, K Januszyk, M L Phillips, et al. *Identifying and characterizing a functional HIV-1 reverse transcriptase-binding site on integrase*, Journal of Biological Chemistry, 2009, 284(12): 7931-7939.

[7] W Liman, N A Lahcen, M Oubahmane, et al. *Hybrid molecules as potential drugs for the treatment of HIV: Design and applications*, Pharmaceuticals, 2022, 15(9): 1092.

[8] M Marra, A Catalano, M S Sinicropi, et al. *New therapies and strategies to curb HIV infections with a focus on macrophages and reservoirs*, Viruses, 2024, 16(9): 1484.

[9] A Chakraborty, G Q Sun, L Mustavich, et al. *Biochemical interactions between HIV-1 integrase and reverse transcriptase*, FEBS Letters, 2013, 587(5): 425-429.

[10] T Ghosh, E J Schwartz, S Ghosh, et al. *Mathematical overview of biochemical and physical interactions considering reverse transcriptase and integrase enzymes to explore HIV progression: A control theoretic approach*, Mathematical Analysis and Applications in Biological Phenomena through Modelling, 2023, 478: 53-68.

[11] S Westerlund. *Dead matter has memory!*, Physica Scripta, 1991, 43(2): 174.

[12] D Baleanu, A Jajarmi, S S Sajjadi, et al. *A new fractional model and optimal control of a tumor-immune surveillance with non-singular derivative operator*, Chaos, 2019, 29(8): 083127.

[13] D Baleanu, P Shekari, L Torkzadeh, et al. *Stability analysis and system properties of Nipah virus transmission: A fractional calculus case study*, Chaos, Solitons & Fractals, 2023, 166: 112990.

[14] A Ebrahimzadeh, A Jajarmi, D Baleanu. *Enhancing water pollution management through a comprehensive fractional modeling framework and optimal control techniques*, Journal of Nonlinear Mathematical Physics, 2024, 31(1): 48.

[15] D Baleanu, A Jajarmi, O Defterli, et al. *Fractional investigation of time-dependent mass pendulum*, Journal of Low Frequency Noise, Vibration and Active Control, 2024, 43(4): 196-207.

[16] T Masuda, O Kotani, M Yokoyama, et al. *Cis-allosteric regulation of HIV-1 reverse transcriptase by integrase*, Viruses, 2022, 15(1): 31.

[17] S G Samko, A A Kilbas, O I Marichev. *Fractional integrals and derivatives: Theory and Applications*, Boca Raton: CRC Press, 1993.

[18] E C de Oliveira, J A T Machado. *A review of definitions for fractional derivatives and integral*, Mathematical Problems in Engineering, 2014, 2014: 238459.

[19] G Kneller, K Hinsen. *Fractional Brownian dynamics in proteins*, The Journal of Chemical Physics, 2004, 121(20): 10278-10283.

[20] M Caputo. *Elasticità e Dissipazione*, Bologna: Zanichelli, 1965.

[21] M Caputo, M Fabrizio. *A new definition of fractional derivative without singular kernel*, Progress in Fractional Differentiation & Applications, 2015, 1(2): 73-85.

[22] A Atangana, D Baleanu. *New fractional derivatives with nonlocal and non-singular kernel: theory and application to heat transfer model*, Thermal Science, 2016, 20(2): 763-769.

[23] A Atangana, I Koca. *Chaos in a simple nonlinear system with Atangana–Baleanu derivatives with fractional order*, Chaos, Solitons & Fractals, 2016, 89: 447-454.

[24] Y Qing, B Rhoades. *T-stability of Picard iteration in metric spaces*, Fixed Point Theory and Applications, 2008, 2008: 418971.

[25] P A Naik, M Yavuz, S Qureshi, et al. *Memory impacts in hepatitis C: A global analysis of a fractional-order model with an effective treatment*, Computer Methods and Programs in Biomedicine, 2024, 254: 108306.

[26] S Qureshi, R Jan. *Modeling of measles epidemic with optimized fractional order under Caputo differential operator*, Chaos, Solitons & Fractals, 2021, 145: 110766.

[27] A Herschhorn, I Oz-Gleenberg, A Hizi. *Quantitative analysis of the interactions between HIV-1 integrase and retroviral reverse transcriptases*, Biochemical Journal, 2008, 412(1): 163-170.

[28] K Das, E Arnold. *HIV-1 reverse transcriptase and antiviral drug resistance. Part 1*, Current Opinion in Virology, 2013, 3(2): 111-118.

[29] A E Taylor, D C Lay. *Introduction to functional analysis*, Krieger Publishing Co., 1986.

[30] F Gao, X Li, W Li, et al. *Stability analysis of a fractional-order novel hepatitis B virus model with immune delay based on Caputo-Fabrizio derivative*, Chaos, Solitons & Fractals, 2021, 142: 110436.

[31] S Marino, I B Hogue, C J Ray, et al. *A methodology for performing global uncertainty and sensitivity analysis in systems biology*, Journal of Theoretical Biology, 2008, 254(1): 178-196.

[32] M McKay, R Beckman. *A comparison of three methods for selecting values of input variables in the analysis of output from a computer code*, Technometrics, 1979, 21(4): 381-402.

[33] D J Hazuda, P Felock, M Witmer, et al. *Inhibitors of strand transfer that prevent integration and inhibit HIV-1 replication in cells*, Science, 2000, 287(5453): 646-650.

[34] O Delelis, K Carayon, A Saïb, et al. *Integrase and integration: biochemical activities of HIV-1 integrase*, Retrovirology, 2008, 5: 114.

[35] S Swindells, J F Andrade-Villanueva, G J Richmond, et al. *Long-acting cabotegravir and rilpivirine for maintenance of HIV-1 suppression*, New England Journal of Medicine, 2020, 382(12): 1112-1123.

[1]Center of Mathematical Biology and Ecology, Department of Mathematics, Jadavpur University, West Bengal, Kolkata-700032, India.
[2]Faculty of Military Science, Stellenbosch University, Private Bag X2, Saldanha 7395, South Africa.
[3]School of Mathematics, Statistics and Mechanics, Beijing University of Technology, Beijing 100124, China.

Email: pritiju@gmail.com